



1 **Is there a bias in AERONET retrievals of aerosol light absorption at low AOD conditions?**

2 Elisabeth Andrews¹, John A. Ogren², Stefan Kinne³, Bjorn Samset⁴

3 ¹CIRES, University of Colorado, Boulder, CO 80309, USA

4 ²NOAA/ESRL/GMD, Boulder, CO 80305, USA

5 ³Max Planck Institute for Meteorology, 20146 Hamburg, Germany

6 ⁴Center for International Climate and Environmental Research – Oslo (CICERO), 0349 Oslo,

7 Norway

8

9 **Abstract**

10 Here we present new results comparing aerosol absorption optical depth (AAOD) and column
11 single scattering albedo (SSA) obtained from in-situ vertical profile measurements with
12 AERONET ground-based remote sensing from two rural continental sites in the US. The profiles
13 are closely matched in time (within +/-3 h) and space (within 15 km) with the AERONET
14 retrievals. These direct comparisons of in-situ-derived to AERONET-retrieved AAOD (or SSA)
15 reveal that AERONET retrievals yield higher aerosol absorption for the low aerosol optical depth
16 (AOD) conditions prevalent at the two study sites. The tendency of AERONET inversions to
17 overestimate absorption at low AOD values is generally consistent with other published
18 comparisons. We conclude that scaling modelled black carbon concentrations upwards to
19 match AERONET retrievals of AAOD may lead to aerosol absorption overestimates in regions
20 of low AOD.

21

22 **1. Introduction**

23 The amount and location of absorbing aerosol in the atmosphere is critical for understanding
24 climate change (e.g., Hansen et al., 1997; Ramanathan and Carmichael, 2008; Bond et al.,
25 2013; Samset et al., 2013). Ramanathan and Carmichael (2008) note the effects of absorbing
26 aerosol (which they termed black carbon (BC)) on atmospheric heating rates, precipitation and
27 weather patterns. (Note: The terminology used to refer to absorbing aerosol is imprecise
28 (Petzold et al., 2013) and encompasses the terms describing chemistry, e.g., 'black carbon'
29 (BC) and terms describing optical effects, e.g., absorption. The measurements reported herein
30 all refer to light absorption.) The vertical distribution of BC can also influence its effect on
31 climate (e.g., Haywood and Ramaswamy, 1998; Samset et al., 2013; Ramanathan and
32 Carmichael, 2008). Single scattering albedo (SSA) is an indicator of the absorbing nature of the
33 aerosol; higher SSA values indicate a more reflective (whiter) aerosol while a more absorbing
34 aerosol will have lower SSA values. SSA is a primary determinant of whether the aerosol will
35 have a warming or cooling effect (e.g., Haywood and Shine, 1995; Hansen et al., 1997; Reid et
36 al., 1998). Uncertainty in the value of SSA due to uncertainties in the amount of absorbing
37 aerosol can even prevent determination of the sign of aerosol forcing on local to regional scales.
38 Bond et al. (2013) assessed BC as the second most important global-average warming species
39 (top-of-atmosphere forcing $+1.1 \text{ W m}^{-2}$, 90% bounds: $+0.17$ to $+2.1 \text{ W m}^{-2}$) after CO_2 (in Bond et
40 al. (2013) the direct effect of BC is 0.71 , 90% bounds: $+0.09$ to 1.26 W m^{-2}).

41



42 Currently, the only way vertical profiles of aerosol absorption can be obtained is via airborne in-
43 situ measurements. Such flights are expensive and tend to primarily occur during intensive
44 field campaigns, which are usually aimed at studying specific aerosol types (e.g., biomass
45 burning, African dust, urban/industrial pollution). This reliance on short-term campaigns results
46 in profile data sets that are sporadic in both space and time, and not necessarily representative
47 of typical conditions. Additional issues with airborne in-situ measurements include adjustment
48 of measurements to ambient conditions, particle losses in sample lines, and instrument
49 uncertainties. Nonetheless, in-situ vertical profiling of absorbing aerosols has provided useful
50 information to modelers trying to understand climate effects, transport, and lifetimes of these
51 important atmospheric constituents (e.g., Koch et al., 2009; Schwarz et al., 2010; Skeie et al.,
52 2011).

53
54 The limited availability of in-situ vertical profile measurements means modelers must rely on
55 globally sparse and/or temporally sporadic airborne measurements to evaluate BC vertical
56 distributions in their models. Alternatively, the column properties retrieved from AERONET
57 measurements and inversions have been widely used to provide a first constraint on modeled
58 vertical aerosol properties (e.g., Sato et al., 2003; Koch et al., 2009; Bond et al., 2013; He et al.,
59 2014; Wang et al., 2014). Use of the AERONET data as an absorption constraint has
60 suggested upscaling of modeled AAOD values by a factor of 2-6 depending on location (e.g.,
61 Bond et al., 2013), although Wang et al. (2016) has shown that better spatial resolution of
62 models and emission inventories can reduce some of the previously observed model/AERONET
63 discrepancies.

64
65 Ground-based remote sensing of both direct attenuation and sky radiances permit inversions of
66 atmospheric column averaged absorption. By retrieving the complex refractive indices at
67 different solar wavelengths as well as the average aerosol size-distribution, absorption related
68 properties can be determined (e.g., aerosol absorption optical depth (AAOD), single scattering
69 albedo (SSA) and, absorption Ångström exponent (AAE)). The AERONET network has a fairly
70 wide spatial coverage on land, with long data records at many sites (Holben et al., 1998;
71 Dubovik et al., 2000; Dubovik and King, 2000). One obvious limitation of the AERONET
72 inversion retrievals is that the uncertainty of the derived single scattering albedo (SSA) becomes
73 very large at low values of AOD (Dubovik et al., 2000). To minimize the effects of this
74 uncertainty, the AERONET Level-2 data invalidates all absorption-related values if the AOD at
75 wavelength 440 nm (AOD_{440}) is below 0.4 (Dubovik et al., 2000; Dubovik et al., 2002; Holben et
76 al., 2006). Unfortunately, this restriction greatly reduces the spatial and temporal coverage of
77 absorption-related data that can be obtained from AERONET. Moreover, by invalidating low
78 AOD cases, the AAOD values that are retained in the AERONET Level-2 data may be biased
79 high.

80
81 Model analysis of global AOD values suggest that 95% of global AOD_{440} values are below 0.4
82 (Figure 1), while 89% of the AOD_{440} values over land are below the 0.4 threshold. Five models
83 in the AeroCom suite have reported daily-average values of AOD_{440} , which can be used to
84 develop a cumulative frequency distribution of the percent of the Earth's surface and days
85 where a Level-2 AERONET retrieval of AAOD might be possible (ignoring the presence of



86 clouds and absence of sunlight). Figure 1 indicates that, at best, Level-2 AERONET AAOD
87 retrievals might represent 5% of the days, globally, and less than 11% of the days over land. In
88 other words, the AOD constraint on Level-2 AERONET almuquantar inversion retrievals means
89 these retrievals represent only a small fraction of the Earth's surface and are biased to
90 conditions of high aerosol loading.

91

92 The other information that Figure 1 provides is the fractional contribution of regions with different
93 AOD_{440} amounts to the total aerosol and the fossil fuel black carbon (BCFF) radiative budget.
94 These values were derived from monthly data from 4 models in the AeroCom suite. The
95 fractional contribution to the radiative budget can be mathematically described as follows: for
96 each model grid box there are three quantities: (i) the radiative forcing ($W m^{-2}$), (ii) the horizontal
97 area of the box (m^2), and (iii) the AOD_{440} . The product of the radiative forcing term and area is
98 the perturbation to Earth's radiative budget due to total aerosol (or BCFF) in the box. The sum
99 of this product over all the boxes is the total perturbation. Figure 1 shows the fraction of the
100 radiative budget perturbation as a function of AOD_{440} . It suggests that approximately 75% of the
101 total aerosol forcing and 83% of BCFF forcing is due to regions of the globe where $AOD_{440} < 0.4$.
102 This highlights the significant contribution of aerosol in these cleaner areas to the total global
103 radiation budget.

104

105 It should be noted that there is significant inter-model variation in the AeroCom cumulative
106 AOD_{440} and radiative forcing plots shown in Figure 1. In particular the BCFF cumulative forcing
107 fraction varies with the lifetime of BC predicted by the models. A long BC lifetime results in more
108 dilute AOD and BCFF radiative forcing distributions. Other issues include the fact that global
109 models have limited spatial and temporal resolution, and generally simulate less variability in
110 aerosol properties than is observed in measurements. However, all models used to generate
111 Figure 1 follow the same general trend as is shown in Figure 1 with the take-away point being
112 that AOD_{440} values > 0.4 are a relatively rare occurrence.

113

114 Because of the potential of the AERONET absorption-related retrievals (e.g., AAOD and SSA)
115 for understanding global distributions of absorbing aerosol, there have been many studies
116 comparing AERONET retrieval values with those obtained from in-situ measurements in order
117 to assess the AERONET retrieval validity. Such comparisons have taken several different
118 forms. There have been direct comparisons where column SSA or AAOD values calculated
119 from individual in-situ vertical profiles have been compared with AERONET retrieved values for
120 retrievals close in time and space (Haywood et al., 2003; Magi et al., 2005; Mallet et al., 2005;
121 Leahy et al., 2007; Corrigan et al., 2008; Osborne et al., 2008; Johnson et al., 2009; Esteve et
122 al., 2012; Schafer et al., 2014). In addition to direct comparisons there have been general,
123 statistical assessments between AERONET and in-situ measurements for both SSA and AAOD
124 including: (a) comparing surface in-situ measurements with AERONET retrievals (e.g., Dubovik
125 et al., 2002; Doran et al., 2007; Mallet et al., 2008; Corr et al., 2009); (b) comparing in-situ SSA
126 (or AAOD) from a few flight segments to the corresponding column SSA (or AAOD) from
127 AERONET (e.g., Kelektoglou et al., 2012; Müller et al., 2012) and (c) comparison of statistical
128 distributions or averages of AERONET retrievals for a given time period with airborne in-situ
129 measurements (e.g., Ramanathan et al., 2001; Leahy et al., 2007; Andrews et al., 2011a;



130 Ferrero et al., 2011; Johnson et al., 2011). Many of these statistical comparisons have shown
131 good agreement between the AERONET and in-situ values. This increased general confidence
132 in the AERONET retrievals. However, such statistical comparisons are not appropriate for the
133 evaluation of the accuracy of individual retrievals.

134

135 The primary scientific question to be addressed in this paper is: *Are the AERONET estimates*
136 *for SSA biased low (or, alternatively, are estimated AERONET AAOD values biased high) under*
137 *low AOD ($AOD_{440} < 0.4$) conditions, or are they just highly uncertain?* The answer to this
138 question may help determine the validity of adjusting model estimates of AAOD to agree with
139 AERONET retrievals (e.g., Sato et al., 2003; Bond et al., 2013). It should be noted that
140 AERONET does not recommend the use of absorption-related parameters (e.g., single
141 scattering albedo, absorption aerosol optical depth, and complex index of refraction) at AOD_{440}
142 below 0.4. Dubovik et al. (2002) suggests the uncertainty of AERONET SSA values more than
143 doubles for AOD_{440} less than 0.2.

144 In what follows, we first evaluate how direct AERONET AAOD retrievals compare with those
145 derived from multi-year, in-situ measurements obtained from vertical profiles over two rural
146 continental AERONET sites in the U.S. Second, we create a summary of all direct AAOD or
147 SSA comparisons between in-situ vs. AERONET data previously presented in the literature in
148 order to place our results about AERONET aerosol absorption-related retrievals in a wider
149 context. Finally, we look at the seasonality of in-situ, AERONET, and modelled (AeroCom) SSA
150 and AAOD values to see if the annual cycles can provide any insight into observed
151 discrepancies in the direct comparisons. Because this study focuses on only two low AOD sites
152 in the continental US which are unlikely to be generally representative of other low loading sites
153 around the globe, and because other factors (e.g., Wang et al., 2016) may contribute to
154 reported differences between modelled and AERONET AAOD we do not attempt to suggest
155 implications for global BC forcing.

156

157 2. Methods

158 This study utilizes data from two sites with collocated AERONET measurements and multi-year,
159 in-situ aerosol profiling measurements. The two sites are Bondville (BND, 40.05°N 88.37°W,
160 230 m asl) and Southern Great Plains (SGP, 36.61°N 97.49°W, 315 m asl). Surface in-situ
161 measurements and AERONET column measurements have been made at both locations since
162 the mid-1990s (e.g., Delene and Ogren, 2002; Sheridan et al., 2001; Holben et al., 1998).
163 Weekly to twice-weekly flights measuring in-situ vertical profiles of aerosol optical properties
164 over these two sites were made for a subset of the years of ground-based observations. At SGP
165 the in-situ profile flights were centered over the site's central facility where the AERONET
166 sunphotometer is deployed. Due to FAA flight restrictions, the BND in-situ profiling flights took
167 place approximately 15 km to the WNW of the AERONET sunphotometer location at the BND
168 surface site (Sheridan et al., 2012). Additionally, for BND, a low level flight leg (200 m agl) was
169 flown directly over the instrumented BND surface site.

170

171 At BND and SGP, the median AOD_{440} values are 0.14 and 0.11, respectively (based on all
172 AERONET Level-2 data from the start of AERONET measurements at each site). These median



173 values fall right around the 50% mark on the AOD cumulative distribution plot (Figure 1),
174 indicating BND and SGP may be appropriate sites to explore potential biases in AERONET
175 AAOD retrievals at lower AOD conditions.
176

177 2.1 IN-SITU

178 The in-situ aerosol profiles were obtained with dedicated Cessna 206 airplanes flying stair-step
179 profiles one to two times per week over the two sites. Between 2006 and 2009, 365 flights were
180 flown over BND (out of a total of 401 flown in the region (Sheridan et al., 2012)), while 171
181 aerosol profile flights were flown over SGP in the 2005-2007 time period (Andrews et al.,
182 2011a). The profiles consisted of 10 (at BND) or 12 (at SGP) level flight legs between
183 approximately 450 and 4600 m asl (corresponding to approximately 150 and 4200 m agl). The
184 profiles, which were 'stair-step' descents, took approximately 2 hours to complete as the
185 airplane spent set amounts of time at each level (10 min/flight level for flight legs above ~1600
186 m asl and 5 min/flight level for flight legs below that altitude) in order to improve measurement
187 statistics. This flight pattern means the last 30 min of the profile were typically in the boundary
188 layer for these two sites and encompassed the majority of the aerosol contribution to column
189 aerosol loading. Descriptions of the flight profiles and aircraft package have been described in
190 detail in other papers (Andrews et al., 2011a; Sheridan et al., 2012) so only a brief description is
191 provided here. Here, we utilize the same 10 flight levels for both profiling sites: 457, 609, 915,
192 1219, 1829, 2439, 3050, 3659 and 4575 m. Of the 365 flights at BND, 253 flights had complete
193 profiles (all flight levels) with valid scattering, absorption and relative humidity data; at SGP, 132
194 flights out of 171 were complete. Only complete profiles were used in this analysis.

195
196 The aircraft were equipped with an inlet that sampled particles with aerodynamic diameter $D_p < 7$
197 μm , and losses in downstream sample lines were estimated to reduce the particle diameter for
198 50% sampling efficiency to 5 μm (Sheridan et al., 2012). Aerosol light absorption (σ_{ap}) was
199 measured at three wavelengths (467, 530, 660 nm) using a Radiance Research Particle-Soot
200 Absorption Photometer (PSAP) and aerosol light scattering (σ_{sp}) was measured at three similar
201 wavelengths (450, 550, 700 nm) using an integrating nephelometer (TSI model 3563). The
202 measurements of absorption and scattering were made at low relative humidity ($\text{RH} < 40\%$).
203 Absorption data were corrected for scattering artifacts, flow and spot size calibrations, etc.,
204 using the Bond et al. (1999) algorithm, with appropriate modifications for wavelength (Ogren,
205 2010). The Anderson and Ogren (1998) correction for instrument non-idealities was applied to
206 the nephelometer data.

207
208 Ambient temperature (T_{amb}) and RH (RH_{amb}) were measured by a sensor (Vaisala Inc, Model
209 Humicap 50Y) mounted on the aircraft fuselage inside a counterflow inlet shroud, and the
210 nephelometer sample pressure was used as a surrogate for ambient pressure. These
211 measurements of ambient meteorological parameters were used to adjust the in-situ optical
212 data to ambient conditions in order to compare with the AERONET measurements and
213 retrievals, which are made at ambient conditions. IMPROVE network surface aerosol chemistry
214 measurements of sulfate and organic carbon (Malm et al., 1994) were utilized to determine a
215 value for the hygroscopic growth parameter ' γ ' for each site based on the Quinn et al. (2005)



216 parameterization. For BND $\gamma=0.71\pm 0.08$, while for SGP $\gamma=0.65\pm 0.08$. At BND the IMPROVE
217 chemistry measurements are co-located at the profile location, while for SGP the measurements
218 at the IMPROVE Cherokee Nation site (approximately 56 km southwest of the profile location)
219 were used. This γ value was then used in conjunction with the airborne RH_{amb} measurements to
220 adjust the in-situ scattering profiles for both SGP and BND.

221

222 The equation used to adjust the dry, in-situ scattering to ambient relative humidity (RH_{amb}) is a
223 commonly used aerosol hygroscopic growth parameterization (e.g., Kasten, 1969; Hanel, 1976;
224 Kotchenruther et al., 1999; Carrico et al., 2003; Crumeyrolle et al., 2014):

225

$$226 \quad \sigma_{sp}(RH_{amb})/\sigma_{sp}(RH_{dry})=a*(1-(RH_{amb}/100))^{-\gamma}. \quad (1)$$

227

228 where $\sigma_{sp}(RH_{amb})$ is the aerosol scattering at ambient RH, $\sigma_{sp}(RH_{dry})$ is the measured scattering
229 at low RH, and γ is the hygroscopic growth parameter derived from the IMPROVE aerosol

230 chemistry. The value of 'a' can be determined using: $a = (1/(1-RH_{dry}/100))^{-\gamma}$ (e.g., Crumeyrolle

231 et al., 2014; Quinn et al., 2005). Here we assume $a=0.9$ based on the typical RH values

232 measured inside the nephelometer for both profile locations (BND $RH_{dry}=12\pm 11\%$; SGP

233 $RH_{dry}=14\pm 10\%$). RH_{amb} at BND and SGP averaged 47.4% and 38.6%, respectively, over all

234 flight levels and seasons (56% (BND) and 43% (SGP) below 1500 m asl). The 95th percentile

235 RH_{amb} values (calculated over all flights and flight levels) were 79.3% and 76.6% at BND and

236 SGP, respectively. (Note: scattering-weighted column average RH values were 54% at BND

237 and 43% at SGP). Applying eq. 1 to the observed RH_{amb} and $\sigma_{sp}(RH_{dry})$ profiles, the average

238 enhancement of column-average σ_{sp} due to hygroscopic growth was 1.52 and 1.36 at BND and

239 SGP, respectively. The corresponding 95th percentiles of column average enhancement of

240 scattering were 2.06 and 2.10.

241

242 The absorption measurements were adjusted to ambient temperature and pressure, but not to
243 ambient RH because the parameterization of the correction and its magnitude are unknown. It
244 is typically assumed that absorbing aerosol is hydrophobic (e.g., Schmid et al., 2003; Reid et al.,
245 2005; Schaefer et al., 2014), i.e., does not take up water. The uncertainties associated with this
246 assumption are discussed in section 2.4.

247

248 Both the scattering and absorption in-situ measurements were adjusted to the two nominal
249 Level-2 AERONET wavelengths in the mid-visible spectrum (440 nm and 675 nm). The 440 nm
250 wavelength is of interest as that is the wavelength for which the AOD constraint for retrieving
251 SSA and hence, AAOD, is given; the 675 nm wavelength is also presented because it is less
252 sensitive to NO_2 , organics, and dust which could potentially bias the in-situ/AERONET
253 comparison. Also, evaluating data at both wavelengths helps in attributing aerosol absorption to
254 BC versus dust, since at 675 nm absorption is almost entirely caused by BC. The measured
255 scattering Ångström exponent was used to adjust the in-situ scattering measurements to the
256 AERONET wavelengths. For the in-situ aerosol absorption wavelength adjustments we used a
257 constant absorption Ångström exponent of 1.2 to minimize the effects of noise in the
258 measurement. Previous studies have shown that for both BND and SGP the absorption



259 Ångström exponent is ~1.0 in the BL and 1.5 at higher altitudes (Andrews et al., 2011; Sheridan
260 et al., 2012). Using the incorrect absorption Ångström exponent will have a negligible effect on
261 the resulting absorption value because of the small difference between the measured and target
262 wavelengths; using an absorption Ångström exponent of 1.2 instead of 1.0 will result in a 1%
263 difference in adjusted wavelength while using an Ångström exponent of 1.2 instead of 1.5 will
264 result in a 2% difference in adjusted absorption.

265
266 Finally, using these in-situ values adjusted to AERONET wavelengths and ambient conditions
267 the column average properties can be determined. Aerosol extinction ($\sigma_{ep} = \sigma_{sp} + \sigma_{ap}$) was
268 calculated and integrated vertically for the profile to obtain the in-situ AOD. The aerosol
269 absorption for each profile was integrated vertically to obtain the in-situ AAOD. The in-situ
270 column SSA (which is compared to the AERONET SSA value in section 3.1) was determined
271 using the AOD and AAOD calculated from the in-situ flights, e.g., $SSA_{col,in-situ} = (AOD_{in-situ} -$
272 $AAOD_{in-situ})/AOD_{in-situ}$). Details of the procedure for calculating the vertical integral are given in
273 Andrews et al. (2004), although, in this study, the in-situ profiles contained two additional high
274 altitude flight levels (at 3659 and 4575 m asl) and the layer at the highest altitude was assumed
275 to extend 457 m above the measurement altitude.
276

277 2.2 AERONET

278 AERONET measurements have been made at BND since mid-1995 and at SGP since mid-
279 1994. The AERONET network makes spectral measurements of aerosol optical depth (AOD)
280 using CIMEL sun/sky radiometers (Holben et al., 1998). The measurements are typically made
281 at seven wavelengths, with an eighth wavelength used for water vapor measurements. The
282 AERONET website (<http://aeronet.gsfc.nasa.gov>) provides links to data from more than 500
283 sites across the globe. The column extinction Ångström exponent (\AA) can be directly calculated
284 from the wavelength-dependent AOD measurements (Eck et al., 1999). In addition to AOD and
285 \AA , algorithms have been developed utilizing both the spectral AOD and the spectral angular
286 distribution of the sky radiances obtained from almucantar scans, which enable retrieval of other
287 column aerosol properties including AAOD, SSA, size distribution, complex refractive index, and
288 fine mode fraction of extinction (FMF_e) (Dubovik and King, 2000; Dubovik et al., 2000; O'Neill et
289 al., 2003; Dubovik et al. 2006). The nominal wavelengths of the almucantar inversion retrievals
290 are 440, 675, 870 and 1020 nm. An additional advantage of the AERONET database is that the
291 retrieval values are obtained consistently – the corrections, QC and algorithms are applied
292 identically for each AERONET location.

293
294 There are different levels of AERONET data available for download from the AERONET
295 website. Level 1.0 is unscreened data while Level-1.5 undergoes automated cloud-screening
296 (Smirnov et al., 2000). Level-2 represents data with pre-field and post-field calibrations applied,
297 manual inspection, and quality assurance (Smirnov et al., 2000). In addition to the Level-1.5
298 screening, the criteria for Level-2 almucantar inversion products include a check of the sky
299 residual error as a function of AOD₄₄₀, solar zenith angle must be greater than or equal 50
300 degrees, and almucantars must have a minimum number of measurements in each of the four



301 designated scattering angle bins. Further, for Level-2 absorption-related products (including
302 SSA, AAOD, AAE, and the complex refractive index) the AOD_{440} must be greater than 0.4 to
303 exclude more uncertain aerosol absorption estimates (Holben et al., 2006).

304

305 The AAOD values reported in the AERONET almucantar inversion files are obtained using the
306 relationship: $AAOD=(1-SSA)*AOD$. Schafer et al. (2014) has a nice description of how SSA is
307 obtained from the AERONET measurements. In the present study, in order to maximize the
308 number of AERONET data points available for comparison with the in-situ measurements,
309 Level-1.5 retrievals of AAOD and SSA were included in the analysis if there was a
310 corresponding valid Level-2 AOD value (i.e., the same primary criterion as was used in Bond et
311 al. (2013)). We will refer to these AAOD and SSA values as 1.5* data.

312 2.3 Merging the IN-SITU and AERONET data sets

313 Merging of collocated (within 15 km), but temporally disparate data sets can induce
314 discrepancies in the combined data set. Lag-autocorrelation analysis (e.g., Anderson et al.,
315 2003) is used to determine an appropriate time window for comparison of the AERONET and in-
316 situ profile measurements. Figure 2 shows that, at the surface at both BND and SGP,
317 scattering is well correlated ($r(k)>0.8$) out to 4-5 hr lag, while absorption is less correlated than
318 scattering. Based on the correlograms, AERONET retrievals were merged with the in-situ
319 profile data when the retrievals were within +/-3 h of the end of the in-situ profile. This is the
320 same time range constraint used to compare AERONET and PARASOL SSA values (Lacagnina
321 et al., 2015).

322 Because the profiles are “stair-step” descents from ~4600 m asl down to ~450 m asl (e.g., see
323 Figure 4 in Sheridan et al., 2012), matching with AERONET retrievals at the end of the profile
324 means that the matches are more closely aligned with when the airplane is in the boundary
325 layer and thus, typically, sampling the highest aerosol concentrations. The boundary layer
326 portion (<1800 m asl) of the ~2 h profile takes approximately 30 min. While the +/- 3 h match
327 window was chosen based on the surface in-situ aerosol lag-autocorrelation statistics (Figure
328 2), other time windows were also examined. For time windows less than +/-3 h (e.g., 1 h and 2
329 h) the fit coefficients (slope, intercept) did not change significantly although the AOD and AAOD
330 correlation coefficients did improve for those smaller time windows. For time windows longer
331 than +/- 3 h (e.g., 6 h and 12h) there were changes in AOD and AAOD fit parameters and the
332 correlation coefficients decreased significantly. For SSA there appeared to be no correlation
333 between AERONET retrievals and in-situ calculated values regardless of match window length
334 (highest SSA correlation coefficient was 0.12, but most were less than 0.05 for both sites). The
335 AERONET/in-situ comparisons for the +/-3 h window are discussed in section 3.1 below.

336 2.4 Uncertainties in IN-SITU and AERONET data

337 In any study comparing parameters obtained from different instruments and/or methods, an
338 understanding of the uncertainties in each of the parameters being compared is critical. Below
339 we discuss the uncertainties inherent in both the in-situ and AERONET datasets.

340 2.4.1 IN-SITU uncertainties



341 Uncertainties for measurements by the in-situ instruments have been described previously (e.g.,
342 Sheridan et al., 2002; Formenti et al., 2002; Shinozuka et al., 2011; Sherman et al., 2015) so
343 only an overview is provided here. Sheridan et al. (2002) calculated uncertainties in aerosol
344 light scattering for the TSI nephelometer to be 7-13% for 10 min legs depending on amount of
345 aerosol present – the higher uncertainty value applies to very low aerosol loadings (scattering <
346 1 Mm^{-1}). We assume that uncertainty in the profile scattering measurements is 13%. 13% is
347 appropriate for the higher altitude flight legs (10 min duration with, typically, low aerosol loading)
348 and is also reasonable for the lower altitude flight legs which are only 5 min in duration but have
349 significantly higher loading. At both BND and SGP the median boundary layer scattering is
350 typically $>10 \text{ Mm}^{-1}$ while median scattering for the upper altitude flight legs is typically between
351 $1\text{-}10 \text{ Mm}^{-1}$ (Andrews et al., 2011; Sheridan et al., 2012).

352
353 Unfortunately, because profile-specific aerosol hygroscopicity measurements were not available
354 for the in-situ aircraft measurements described here, a single hygroscopic growth
355 parameterization was applied for all profiles at each site as described in Section 2.1 and
356 equation 1. To determine the uncertainty in AOD induced by the uncertainty in the scattering
357 adjustment to ambient RH, AOD values were calculated using different γ values representing
358 the range of hygroscopic growth factors suggested by the aerosol chemistry. Specifically,
359 AOD_{440} was calculated for $\gamma \pm 1$ standard deviation and $\gamma \pm 2$ standard deviations. Using this
360 approach, the uncertainty in AOD due to adjustment to ambient RH was determined to be
361 between 9% and 16%. This uncertainty might seem to be low, but recall that the 95th
362 percentiles of ambient RH values observed throughout the profiles were ~80% but that more
363 typically ambient RH in the boundary layer was less than 70% at BND and less than 60% at
364 SGP. Sum of squares uncertainty analysis suggests the overall uncertainty in the in-situ AOD is
365 approximately 30% for higher ambient humidities ($\text{RH}_{\text{amb}} > 70\%$) and approximately half that at
366 $\text{RH}_{\text{amb}} < 50\%$.

367
368 The PSAP measurement of aerosol absorption is more uncertain than the aerosol scattering
369 measurements – PSAP uncertainty is reported to be in the 20-30% range (e.g., Bond et al.,
370 1999; Sheridan et al., 2002; Sherman et al., 2015). It should be noted that the PSAP absorption
371 measurement represents all absorbing aerosol collected on its filter, as opposed to being
372 specific to 'black carbon' absorption. That is actually helpful for this particular study as the
373 AERONET retrieval of AAOD also represents all flavors of absorption (e.g., 'black carbon',
374 'brown carbon' and dust).

375
376 There is, however, some question of whether the PSAP (or any filter-based measurement) is
377 able to accurately represent absorption by particles coated with semi-volatile or liquid organics,
378 due to the possibility of such coatings changing the characteristics of the filter substrate
379 (oozing!) after impaction (e.g., Subramanian et al., 2007; Lack et al., 2008). The effects of such
380 oozing are to increase the absorption value reported by the PSAP relative to that reported by a
381 non-filter-based instrument (Lack et al., 2008); in other words the aerosol absorption values
382 obtained from PSAP measurements may have a positive bias. It is worthwhile to explore the
383 potential magnitude of such a bias. The mean mass concentrations of organic aerosol
384 determined from the IMPROVE measurements near BND and SGP (the OCf value in the



385 IMPROVE data set; Malm et al., 1994) are similar for both sites and less than $2 \mu\text{g}/\text{m}^3$, putting
386 them firmly in the rural/remote category identified by Lack et al (2008; their figure 4). Depending
387 on whether figure 3 or figure 4 in Lack et al. (2008) is used, Lack et al.'s (2008) results suggest
388 that the PSAP might be overestimating absorption by a factor of 1.1 to 1.5 due to artifacts
389 caused by organic aerosols. However, in a subsequent study, Lack et al. (2012) reported a
390 PSAP overestimate by factors of 1.02-1.06 over Los Angeles, considerably lower than the Lack
391 et al. (2008) results.

392

393 The positive bias in absorption related to filter-based measurements is the same order of
394 magnitude and direction of the absorption enhancement factor found by some lab and
395 theoretical studies for coated absorbing particles suspended in the atmosphere. Absorption
396 enhancement values of 1.3-3 have been predicted for coated particles (e.g., Bond et al., 2006;
397 Lack et al., 2009; Cappa et al., 2012) although enhancements larger than a factor of 2 have not
398 been measured for ambient aerosol (e.g., Lack et al., 2008; Cappa et al., 2012; McMeeking et
399 al., 2014). Wang et al. (2014) suggested that an absorption enhancement factor of 1.1 was
400 appropriate for fossil fuel influenced aerosol and that 1.5 was a more reasonable enhancement
401 factor for biomass burning affected aerosol. Biomass burning does not have a consistent
402 influence on either BND or SGP. Cappa et al. (2012) suggested that the discrepancies between
403 ambient and modelled and/or laboratory results, could be a result of differences in particle
404 morphology and/or chemistry. We have not made any adjustments for the absorption effects of
405 coatings or the potential positive bias in PSAP measurements as (a) the science is still unclear
406 and (b) additionally, measured absorption Ångström exponents are quite low (close to 1)
407 suggesting little influence of coatings.

408

409 In addition to the potential absorption enhancement due to organic coatings, it has been
410 suggested that aerosol water on absorbing particles may also enhance absorption. There have
411 been very few studies where the hygroscopic growth enhancement of absorption was explicitly
412 considered. Redemann et al. (2001) modeled absorption enhancement as a function of RH
413 based on characteristic atmospheric particles and found absorption enhancement values of up
414 to 1.35 at 95% RH; for the 95th percentile RH_{amb} values encountered at BND (78.9%) and SGP
415 (76.6%), the Redemann et al. (2001, their figure 2) study would predict absorption
416 enhancements of ~ 1.1 . Nessler et al. (2005) and Adam et al. (2012) utilized both ambient
417 aerosol measurements and Mie theory to calculate absorption enhancement values due to
418 hygroscopic water uptake. Nessler et al. (2005) does not provide absorption enhancements as
419 a function of RH, but Adam et al. (2012) suggest absorption enhancements due to hygroscopic
420 growth of less than 1.1 at 80% humidity. Brem et al. (2012) report on laboratory studies that
421 show that aerosol absorption was enhanced by a factor of 2.2 to 2.7 at 95% relative humidity
422 relative to absorption at 32% relative humidity, although for RH less than $\sim 80\%$ (i.e., the RH
423 values observed in this study) they show no absorption enhancement (their figure 9). Lewis et
424 al. (2009) actually observe a decrease in absorption with increasing RH for some biomass fuels,
425 but hypothesize the decrease might have been due to their measurement technique and/or a
426 change in the morphology of the particles.

427



428 In summary, the positive bias in the PSAP measurements of aerosol light absorption might be
429 as high as a factor of 1.1 to 1.5 due to oozing (e.g., the overestimate of absorption reported by
430 Lack et al., (2008) for filter-based measurements). Atmospheric absorption may be
431 underestimated by PSAP measurements by up to a factor of 1.5 due to not accounting for
432 coating (organic or water) effects. Without additional laboratory and field measurements to
433 quantify the net effect of the possible positive and negative biases in PSAP measurements of
434 aerosol light absorption, it is not possible to estimate the actual uncertainty in the in-situ light
435 absorption measurements reported here due to coating effects.

436

437 Once the uncertainties in the in-situ aerosol scattering and absorption are known, the
438 uncertainty in SSA ($SSA = \sigma_{sp} / (\sigma_{sp} + \sigma_{ap})$) can also be calculated. Formenti et al. (2002, their
439 equation 5) suggests the uncertainty in single scattering albedo ($\delta SSA / SSA$) can be calculated:

440

$$441 \quad \delta SSA / SSA = (1 - SSA) * [(\delta \sigma_{sp} / \sigma_{sp})^2 + (\delta \sigma_{ap} / \sigma_{ap})^2]^{1/2} \quad (2)$$

442

443 For scattering uncertainties of 30%, (combined nephelometer and f(RH) induced uncertainty),
444 PSAP absorption uncertainties of 25%, and SSA values of 0.9, equation 2 results in an in-situ
445 SSA uncertainty of ~4% or approximately 0.04.

446

447 In addition to instrumental uncertainties there are also uncertainties associated with the aircraft
448 flight patterns, i.e., the presence of aerosols below, between and above the discrete flight levels.
449 Several papers (Andrews et al., 2004; Esteve et al., 2012; Sheridan et al., 2012) have shown
450 that there is a high correlation ($R^2 > 0.8$) between scattering measured at the surface site (SGP
451 or BND) with scattering measured at the corresponding lowest flight leg, although the slopes of
452 the relationships indicated that the airplane measurements might be missing a fraction (10-20%)
453 of the aerosol below about 150 m agl. Additionally, Esteve et al. (2012) found high correlation
454 (slope=1.01, $R^2 \sim 0.7$) between scattering AOD calculated by assuming the lowest leg
455 represented scattering in the entire layer between surface and that flight leg with scattering AOD
456 calculated from 1-sec data obtained during descent from the lowest flight leg to landing. This
457 result suggested that no consistent bias would result from assuming the lowest flight leg was
458 representative of the aerosol between surface and that altitude. Similarly, Esteve et al. (2012)
459 investigated differences in aerosol scattering between and at flight levels by comparing
460 scattering AOD from the airplane descent between layers with that calculated from the individual
461 level legs in the profile. Again they were able to confirm that measurements made during the
462 fixed flight altitudes are representative of the aerosol near those altitudes. Different approaches
463 have been used to assess whether aerosol loading contributions above the highest flight level
464 (4.6 km asl) are important Andrews et al. (2004) utilized Raman lidar measurements to
465 determine that 80-90% of the aerosol was below 3.7 km asl at SGP (3.7 km was the maximum
466 altitude flown by the original SGP airplane, although all the profile flights utilized here occurred
467 after the maximum flight level was increased to 4.6 km asl). For BND, Esteve et al. (2012)
468 noted that CALIPSO data indicated negligible extinction above 4.6 km asl.

469

470 *2.4.2 AERONET uncertainties*



471 Uncertainties in AERONET retrievals have been reported in several papers. Eck et al. (1999)
472 indicate that the uncertainty in AOD is approximately 0.01 for a field-deployed AERONET
473 sunphotometer at solar zenith angle = 0 (i.e., sun directly overhead). For the almucantar
474 retrievals (solar zenith angle > 50) used here, the AOD uncertainty will be smaller as the
475 uncertainty in AOD decreases inversely with air mass (Hamonou et al., 1999; their equation 1).
476 Dubovik et al. (2000) report AERONET retrieved SSA uncertainties in their Table 4. For water
477 soluble aerosol (the predominant aerosol type at both BND and SGP) they report that SSA
478 values are reliable to within ± 0.03 when $AOD_{440} > 0.2$, while the uncertainty in SSA increases to
479 (± 0.05 - 0.07) for $AOD_{440} \leq 0.2$. The almucantar retrieval of SSA may be biased by errors in the
480 surface reflectance when the AOD is very low. Mallet et al. (2013) reports an AAOD uncertainty
481 of 0.01 but does not indicate whether or how the AAOD uncertainty would change with AOD_{440} .
482 Using the sum of squares propagation of errors to calculate the uncertainty in AAOD for both
483 high and low AAOD cases results in an AAOD uncertainty of approximately ± 0.015 for both high
484 and low AOD cases (high $AOD_{440}=0.5$, $\delta AOD=0.01$, $SSA=0.95$, $\delta SSA=0.03$, $AAOD=0.026$; low
485 $AOD_{440}=0.2$, $\delta AOD=0.01$, $SSA=0.95$, $\delta SSA=0.07$, $AAOD=0.011$). An AAOD uncertainty value of
486 ± 0.015 suggests an uncertainty of about 60% in AAOD for $AOD_{440}=0.5$ and more than 140%
487 uncertainty in AAOD for $AOD_{440}<0.2$.

488 3. Results

489 In this section we first present comparisons of AOD, AAOD and SSA from the in-situ
490 measurements at BND and SGP with AERONET retrievals. This includes (1) direct
491 comparisons of each in-situ profile with contemporaneous AERONET retrievals; the BND and
492 SGP comparisons are then put in the wider context of a literature review of similar direct
493 comparisons of in-situ and AERONET AAOD and SSA; (2) seasonal comparisons of AOD,
494 AAOD and SSA from Phase II AeroCom model results, AERONET retrievals and in-situ
495 measurements for BND and SGP; and finally, (3) we discuss these results in the context of
496 biases in determination of AAOD.

497

498 *3.1.1 BND and SGP: in-situ vs AERONET – Direct Comparisons*

499 Figures 3, 4 and 5 show the direct comparisons of AOD, AAOD and SSA at both 440 nm and
500 675 nm. Table 1 provides a comparison of the statistical values (median, mean and standard
501 deviation) at 440 nm for each of the parameters at both of the sites for these direct
502 comparisons. Depending on atmospheric conditions, there may be more than one AERONET
503 retrieval within +/-3 hours of the end of each profile, which is why there are more data points
504 plotted than there are flights.

505

506 The comparison between in-situ and AERONET AOD is important because it can be used to
507 evaluate how well the in-situ and AERONET retrievals can be expected to agree and, thus, set
508 the context for the AAOD and SSA comparisons. Many studies have investigated the
509 relationship between in-situ and remotely sensed AOD (e.g., Crumeyrolle et al., 2014; Schmid
510 et al., 2009, and references therein). As noted in these studies, the in-situ derived AOD values
511 tend to be slightly lower than the AOD retrieved from remote sensing measurements. Figure 3
512 presents the comparison of Level-2 AOD for AERONET and in-situ measurements at 440 nm
513 and 675 nm for two sets of AERONET AOD data. The first comparison (red points on plots) is



514 for all direct sun AERONET Level-2 AOD measurements. The second comparison (blue points
515 on plots) is for AERONET Level-2 AOD measurements where all the criteria required for
516 almucantar retrievals are satisfied. Table 2 summarizes how many points make up each of
517 these data sets.

518

519 In general, Figure 3 shows that AERONET AOD tends to be higher than the in-situ AOD,
520 although there is good correlation between AERONET and in-situ AOD. The correlation
521 coefficients (R^2) are within the range we would expect based on the lag-autocorrelation of
522 scattering at these two sites (Figure 2) and the ± 3 h time window. The correlations improve for
523 the more restrictive Level-2 almucantar retrievals. The lower in-situ AOD values observed at
524 both sites, compared to AERONET, may be due to the hygroscopicity adjustment from dry in-
525 situ to ambient RH conditions being too low or undersampling of larger particles (e.g., Esteve et
526 al., 2012). Esteve et al. (2012) found slopes closer to 1 when they restricted AERONET/in-situ
527 AOD comparison to low ambient RH ($<60\%$) conditions, although the AERONET AOD values
528 were still larger than the in-situ AOD. The effect of undersampling larger particles or
529 underestimating aerosol hygroscopicity on the AAOD and SSA comparisons are discussed in
530 section 3.1.2. The relationships observed between AERONET and in-situ AOD for both sites
531 are very similar to those observed for the recent DISCOVER-AQ campaign (e.g., Crumeyrolle
532 et al., 2014, their figure 3).

533

534 Figure 4 presents the comparison of AAOD for AERONET and in-situ measurements. As
535 described above, the AERONET AAOD values shown in Figure 4 are what we have termed
536 Level-1.5* data – i.e., they are from Level-1.5 almucantar retrievals when there was a valid
537 Level-2 almucantar retrieval, but the $AOD_{440} > 0.4$ constraint was not applied. In contrast to the
538 AOD comparison depicted in Figure 3, the AERONET Level-1.5* AAOD values are significantly
539 higher than the in-situ AAOD values. Figure 4 also shows that the correlation between the
540 AERONET and in-situ AAOD is poorer than it was for AOD, particularly at BND (R^2 is 0.34 at
541 BND and 0.77 at SGP for the 440 nm comparison). The poor correlation at BND is somewhat
542 surprising given the lag-autocorrelation results for aerosol absorption (Figure 2a) at the BND
543 surface site. Both Figure 4 and the median values provided in Table 1 indicate that AERONET
544 Level-1.5* AAOD tends to be larger than the in-situ AAOD, although the scatter in the
545 relationships (particularly at BND) suggests that a multiplicative factor doesn't represent the
546 relationship very well. The purple points in Figure 4 indicate AAOD retrievals where the
547 $AOD_{440} > 0.2$. There is no obvious improvement of the relationship between in-situ and
548 AERONET AAOD when these points are considered (although there are only 6-7 comparison
549 points above $AOD_{440} > 0.2$ for each site).

550

551 The AAOD comparisons at 675 nm at BND (Figure 4c) are quite similar to those at 440 nm,
552 suggesting that there is little contribution to absorbing aerosol from dust, organic carbon and/or
553 NO_2 . In contrast, at SGP, there is a change in the relationship between AERONET and in-situ
554 AAOD from 440 to 675 nm indicating that one or more of these components may affect the 440
555 nm comparisons at that site (Figure 4d). Ångström exponent values from the matched
556 AERONET and in-situ profile data do not support the presence of dust, while the rural nature of
557 the site suggests significant levels of NO_2 are unlikely. Thus the most likely explanation is the



558 presence of organic carbon, although the IMPROVE sulfate and organic data used to estimate
559 aerosol hygroscopicity do not support this. The IMPROVE measurements tend to suggest a
560 relatively small contribution of organics to the aerosol mass with the average mass
561 concentration of organics only 40 to 60% that of sulfate aerosol mass concentration for BND
562 and SGP, respectively. In contrast, the Aerosol Chemical Speciation Monitor (ACSM)
563 measurements by Parworth et al. (2015) indicate that, depending on the month, organic aerosol
564 can contribute up to 70% of the total aerosol mass at SGP.

565

566 Figure 5 presents the comparison of column SSA retrieved from AERONET inversions (Level-
567 1.5* data) with the column SSA calculated from in-situ profile measurements of aerosol
568 scattering and absorption at BND and SGP. Consistent with the AOD and AAOD comparisons
569 (Figures 3 and 4) the SSA retrieved from AERONET tends to be much lower than the SSA
570 calculated from the in-situ profile measurements. At both sites the range in AERONET-retrieved
571 SSA is much wider than the range in column SSA obtained from the in-situ profiles. Long term,
572 in-situ measurements at the BND and SGP surface sites yield mean SSA values of 0.92 and
573 0.95 respectively (Delene and Ogren, 2002, based on monthly-averaged data). Delene and
574 Ogren's (2002) surface SSA values are reported at low RH (RH<40%) and 550 nm; adjusting
575 them to ambient conditions and 440 nm would likely cause them to increase making them more
576 comparable to the in-situ column SSA depicted in Figure 5 but even less like the AERONET
577 Level-1.5* SSA values. As with Figure 4, the purple points on Figure 5 indicate when the
578 $AOD_{440} > 0.2$; there does not appear to be an improvement in the relationship between in-situ
579 and AERONET SSA when only these purple points are considered.

580

581 *3.1.2 How might AOD discrepancies affect SSA and AAOD comparisons?*

582 Figure 3 shows that the AERONET AOD may be slightly larger than the in-situ AOD, while
583 Figures 4 and 5 suggest that the AERONET retrievals significantly overestimate the amount of
584 absorbing aerosol (low SSA, high AAOD) relative to the in-situ measurements. The slight
585 deviation between in-situ and AERONET AOD may lead to questions about whether directly
586 comparing other AERONET and in-situ parameters (e.g., SSA, AAOD) is a reasonable thing to
587 do and whether the AAOD and SSA comparisons shown in Figures 4 and 5 are related to
588 issues with the AOD comparison. As mentioned above, Esteve et al. (2012) suggested the
589 AOD difference was most likely due to either underestimating the hygroscopic growth correction
590 and/or undersampling of supermicron particles by the aircraft inlet. In this section we evaluate
591 how these two possible causes of the AOD discrepancy might affect the SSA and AAOD
592 comparisons.

593 Increasing the hygroscopic growth adjustment of the in-situ measurements would enhance the
594 in-situ scattering values used to calculate the in-situ AOD, but would not change the in-situ
595 AAOD because the absorbing particles are assumed to be non-hygroscopic. Consequently, the
596 comparison depicted in Figure 4 would not change with a different adjustment for hygroscopic
597 growth. Increasing the in-situ AOD, without affecting the in-situ AAOD, would result in higher in-
598 situ SSA values and an even greater discrepancy between AERONET and in-situ SSA values
599 than shown in Figure 5.

600



601 The other likely candidate to explain the in-situ AOD being slightly lower than the AERONET
602 AOD is aircraft under-sampling of super-micron aerosol particles. Esteve et al.'s (2012)
603 comparison of column in-situ and AERONET scattering Ångström exponents at BND suggested
604 that the airplane measurements might be under-sampling larger particles. Sheridan et al.
605 (2012) estimated that the aircraft inlet 50% cut-off diameter is approximately 5 μm , so particles
606 larger than that are unlikely to be sampled by the in-situ measurements but will be sensed by
607 the AERONET sunphotometer. The AERONET volume size distributions were used to estimate
608 the fraction of column extinction due to particles less than 5 μm . At BND the mean and
609 standard deviation of the 5 μm extinction fraction ($\text{extinction}(D<5\mu\text{m})/\text{extinction}(D<30\mu\text{m})$) was
610 0.94 ± 0.06 , while at SGP the extinction fraction value was 0.90 ± 0.07 . At the BND and SGP
611 surface sites, most (80-90%) of the observed sub-10 μm scattering and absorption is also
612 attributed to sub-micron aerosol, with absorption more likely to be in the sub-micron size range
613 than scattering (Delene and Ogren, 2002; Sherman et al., 2015). This is consistent with the
614 observation that absorbing aerosol tends to be concentrated in sub-micron particles for typical
615 aged continental air masses (e.g., Hinds, 1982). Based on these observations, larger and
616 primarily scattering particles are more likely to be under-sampled by the in-situ measurements
617 than absorbing particles. This is the opposite of what is needed to explain the discrepancies
618 between AERONET and in-situ AOD, AAOD, and SSA shown in Figures 3-5. The in-situ
619 measurements would need to preferentially under-sample absorbing aerosol relative to
620 scattering aerosol in order to come into line with the AERONET observations.

621

622 Additionally, Sheridan et al. (2012) calculated particle transmission losses from behind the
623 sample inlet on the airplane to both the nephelometer and PSAP to be similar and to be less
624 than 10% in the particle diameter range $0.01 < D < 1 \mu\text{m}$. This suggests that preferential losses of
625 absorbing aerosol are also unlikely to occur downstream of the aerosol inlet.

626

627 3.2 Literature survey: in-situ vs AERONET – Direct Comparisons

628 Direct comparisons at BND and SGP suggest that AERONET retrievals underestimate SSA
629 and, consequently, that AERONET overestimates AAOD relative to in-situ measurements of
630 AAOD for the low AOD conditions typical at these two sites. The next question to address is
631 whether this bias, found for two rural, continental sites in the central US with relatively low
632 aerosol loading, is more widely observed for direct in-situ/AERONET comparisons at a variety of
633 sites/conditions. As in section 3.1, the focus in this section is on direct comparisons of column-
634 averaged SSA (or AAOD) derived from in-situ measurements made during aerosol profiling
635 flights that were flown in close proximity (temporal and spatial) to an AERONET retrieval. Tables
636 3 and 4 summarize literature results describing the direct comparisons of AERONET retrievals
637 with in-situ aerosol profile measurements for AAOD and column SSA. Figure 6 provides a
638 graphical overview of the SSA comparisons described in Table 4. Tables 3 and 4 and Figure 6
639 also include the BND and SGP comparisons described in this study. With the possible
640 exception some of the profiles reported by Corrigan et al. (2008), the literature comparisons
641 cited in Tables 3 and 4 and shown in Figure 6 have been made at higher AOD conditions
642 ($\text{AOD}_{440} > 0.3$) to reduce retrieval uncertainty. In contrast, the SGP and BND comparisons are



643 more representative of global AOD (Figure 1) with the majority of the comparisons at BND and
644 SGP occurring for $AOD_{440} < 0.2$.

645

646 Tables 3 and 4 have been restricted to studies with direct comparisons of column-averaged
647 AAOD or SSA retrieved from full in-situ vertical profiles flown near (within ~100 km) AERONET
648 sites within a few hours of the AERONET retrieval, i.e., studies that are comparable to the BND
649 and SGP studies described in Section 3.1. Included in the tables are the field campaign name
650 (if applicable), number of AAOD or SSA comparisons, the primary type of aerosol studied,
651 summary of AOD comparisons (if available), instruments and data processing (e.g., instrument
652 corrections, treatment of hygroscopicity, wavelength adjustment) and a summary of the results
653 of the AAOD comparison. The last column in Tables 3 and 4 includes information on the spatial
654 and temporal differences between the in-situ measurements and AERONET retrievals and
655 comments on treatment of the AERONET data. It should be noted that the number of SGP and
656 BND comparisons of AAOD and SSA in Tables 3 and 4 are only possible because we've utilized
657 AERONET retrievals below the recommended threshold of $AOD_{440} > 0.4$. The uncertainty for the
658 BND and SGP comparisons is much higher than for some of the other direct comparisons due
659 to the low AOD conditions observed at these sites.

660

661 For the three AAOD closure studies listed in Table 3 (the BND and SGP results presented here,
662 plus results from a field campaign over the Indian Ocean) the AERONET retrievals indicate
663 more absorbing aerosol in the column than is suggested by the corresponding in-situ
664 measurements. The Corrigan et al. (2008) paper mentioned in Table 3 is the sole
665 AERONET/in-situ AAOD comparison cited by Bond et al. (2013), as it was the only published
666 direct AAOD comparison available. Corrigan et al. (2008) present no AOD comparisons that
667 could provide an indication of their sampling system efficiency, and information about the
668 wavelength of the comparisons and profiles specifics are lacking. To our knowledge, no other
669 direct comparisons of in-situ and AERONET AAOD are available in the literature.

670

671 The SSA comparison studies listed in Table 4 and visually summarized in Figure 6 indicate that,
672 even at higher AOD, AERONET has a bias towards more-absorbing aerosol (lower SSA)
673 relative to in-situ measurements. While much of the observed difference between $SSA_{in-situ}$ and
674 $SSA_{AERONET}$ may fall within the uncertainty of the SSA values, as noted in Schafer et al. (2014),
675 the fact that the difference ($SSA_{AERONET} - SSA_{in-situ}$) is predominately negative across all the
676 direct comparisons found in the literature is not what would be expected from random error.

677

678 Most of the SSA comparisons in Table 4 found fairly good agreement between AERONET and
679 in-situ AOD, suggesting that the issue is an over-estimation of the absorption contribution to
680 AOD rather than an underestimation of the AOD scattering contribution. This is consistent with
681 the AERONET AAOD values being greater than those obtained from in-situ measurements
682 presented in Table 3. Out of the 63 profiles compared in Table 4, there are eight exceptions,
683 (three from Leahy et al. (2007) and five from this study for the BND site) where $SSA_{AERONET}$ is
684 larger than the corresponding $SSA_{in-situ}$. Interestingly, the three exceptions from Leahy et al.
685 (2007) were for their high AOD ($AOD_{550} > 0.6$) cases; for their two low AOD ($AOD_{550} < 0.3$) cases
686 the opposite was found, i.e., $SSA_{AERONET} < SSA_{in-situ}$.



687

688 In summary, the literature survey featuring measurements across the globe for many aerosol
689 types suggests that even at higher AOD conditions, direct comparisons of AERONET with in-
690 situ aerosol profiles find that AERONET column SSA is consistently lower than the SSA
691 obtained from in-situ measurements (although often within the uncertainty of the AERONET
692 SSA retrieval). If there was no bias in the AERONET retrieval we would expect
693 (AERONET_SSA – INSITU_SSA) to be evenly distributed around zero. Instead, the results
694 from the literature suggest either that AERONET is biased towards too much absorption, or that
695 in-situ measurements undersample aerosol absorption.

696 An alternative explanation is that the AERONET SSA uncertainties are non-symmetric. Dubovik
697 et al. (2000) suggest that simulated retrievals of SSA for ‘water soluble aerosol’ are asymmetric
698 when different ‘instrumental offsets’ are assumed, particularly at lower AOD values (0.05 and
699 0.2). Their figure 4 shows a much larger decrease in SSA for some instrumental offsets relative
700 to the increase in SSA observed for an instrumental offset of the same magnitude but opposite
701 sign. Asymmetry is also indicated for ‘biomass burning’ aerosol (their figure 7) although the
702 asymmetry is in the opposite direction, i.e., the increase in SSA is larger than the decrease for a
703 given pair of instrumental offset values. It is not obvious from their figure 7 whether the retrievals
704 are asymmetric for simulated dust aerosol. Interestingly, at least four of the points in Figure 6
705 with AERONET_SSA > INSITU_SSA (three of the Leahy et al. (2007) points and the BND point
706 with AOD ~0.4) represent retrievals of biomass burning aerosol.

707 3.3 BND and SGP: in-situ vs AERONET and AeroCom model output – Statistical Comparisons

708 Most of the statistical comparisons between AERONET and in-situ profiles (e.g., Ramanathan et
709 al., 2001; Leahy et al., 2007; Ferrero et al., 2011; Johnson et al., 2011) were for short-term field
710 campaigns with a limited number of in-situ profiles. The advantage of the multi-year, in-situ
711 vertical profiling programs at BND (401 flights) and SGP (302 flights) is that we can compare the
712 statistics for both in-situ and AERONET values as opposed to comparing individual in-situ
713 values to remote retrieval statistics. Figure 1 in Andrews et al. (2011) and Figure 9 in Sheridan
714 et al. (2012) demonstrate that the BND and SGP flight programs captured the multi-year
715 seasonality in aerosol properties at these two sites. Because of the large number of flights over
716 an extended period of time, Skeie et al (2011) was able to compare the seasonally averaged, in-
717 situ absorbing aerosol profiles from BND and SGP with seasonal vertical profiles of black
718 carbon generated by the Oslo-CTM2 model. Skeie et al (2011) found that the model
719 underestimated absorbing aerosol relative to the BND and SGP in-situ profiles for most seasons
720 and altitudes, although agreement between the model and measurements tended to be better at
721 higher altitudes.

722

723 As mentioned in the introduction, AERONET retrievals of AAOD have been used to suggest
724 upscaling factors for modelled values of absorbing aerosol (e.g., Sato et al., 2003; Bond et al.,
725 2013). These model/AERONET comparison studies are typically based on model and
726 measurement statistics (i.e., properties are averaged over time and region) rather than direct
727 comparisons due to both computational constraints and the discrete nature of the AERONET
728 measurements. Given the statistical nature of some historical AERONET/in-situ comparisons



729 as well as the typical model/AERONET comparison constraints, in this section we compare
730 monthly statistics for in-situ measurements, AERONET retrievals and AeroCom model output.

731

732 Figure 7 shows the 440 nm monthly medians of AOD, AAOD and SSA at BND and SGP based
733 on the in-situ profile measurements, and two versions of AERONET retrievals as described
734 below. For the in-situ properties, all profiles were used, regardless of whether there was an
735 AERONET retrieval corresponding to the flight. The AERONET monthly medians in Figure 7
736 use the long-term (1996-2013) AERONET data record for each site. As described previously,
737 the lines labeled AERONET 1.5* were calculated from Level-1.5 inversion data with matching
738 Level-2 almucantar retrievals. The lines labeled AERONET 2.0 utilized only Level-2 almucantar
739 retrieval data. In both cases the median AERONET AOD values represent those Level-2 AOD
740 measurements for which there was also an AAOD and SSA retrieval, ensuring that the
741 AERONET AOD medians represent the same set of retrievals as the corresponding AAOD and
742 SSA medians in the figure. The AERONET Level-1.5* AOD monthly medians are representative
743 of the direct sun AERONET Level-2 AOD climatology at the two sites. Figure 7 also includes
744 the AeroCom Phase II model monthly medians (Kinne et al., 2006, Myhre et al., 2013) with
745 model emissions, meteorology and other details briefly described in Myhre et al. (2013). The
746 AeroCom values, which were provided at 550 nm, have been adjusted to 440 nm using the
747 reported AeroCom monthly scattering Ångström exponent to adjust AOD wavelength and
748 assuming an absorption Ångström exponent of 1 for the AAOD wavelength adjustment. It
749 should be noted that the three monthly data sets (AERONET, AeroCom, and in-situ) plotted in
750 Figure 7 are derived from measurements for overlapping, but not identical time periods, i.e.,
751 these plots represent climatological comparisons rather than direct comparisons of the data
752 sets.

753

754 At both sites, the climatological seasonal patterns for AOD (i.e., high in summer, low in winter)
755 are similar for the three data sets: in-situ measurements, AERONET Level-1.5* retrievals (recall
756 that the AERONET 1.5* AOD is representative of the overall AERONET AOD climatology at
757 each site) and AeroCom model output. At BND the AeroCom model AOD tends to be larger
758 than the in-situ and AERONET 1.5* AOD values by up to a factor of two. AERONET 1.5* AOD
759 is larger than the in-situ AOD in the summer (by up to 50%) but quite close the rest of the year
760 (typically within 20%). At SGP the AOD monthly medians from in-situ measurements and
761 AERONET Level-1.5* are almost identical for August-December, with slightly more discrepancy
762 among the AOD values in summer and early part of the year. In contrast, AeroCom model
763 median AOD values tend to agree better with AERONET 1.5* and in-situ AOD values from
764 January-July but are noticeably higher (up to a factor of 2) in the later half of the year. At both
765 sites, the median AERONET Level-2 AOD values (corresponding to AAOD and SSA retrievals)
766 are much higher (by a factor of 2 or more) than the Level-1.5* and in-situ climatologies due to
767 the $AOD_{440} > 0.4$ constraint. During the cleanest months of the year (December-February) there
768 are none to few Level-2 almucantar retrievals of SSA and AAOD at either BND or SGP.

769

770 For AAOD at BND, the AeroCom model output falls between the AERONET 1.5* and in-situ
771 values, with AERONET 1.5* AAOD being higher than the in-situ data by up to a factor of 8. As
772 with AOD, the AERONET AAOD Level-2 values are much higher than the in-situ or modelled



773 AOD values due to the constraint that they are only retrieved at high loading conditions
774 ($AOD_{440} > 0.4$). The three data sets (AeroCom, in-situ and AERONET 1.5*) agree best in the
775 month of May when the median values of AAOD are within 30%. At SGP there is fairly good
776 agreement between AeroCom model and in-situ AAOD for the first 7 months of the year, while
777 the AERONET 1.5* monthly AAOD values are considerably higher for that same time period.
778 For the latter part of the year the in-situ AAOD values tend to be lower than both AERONET and
779 AeroCom AAOD values.

780

781 The AERONET 1.5* SSA values tend to be quite a bit lower than the other data sets at both
782 sites, which is why the AERONET 1.5* AAOD values tend to be higher (recall that for
783 AERONET data AAOD is calculated using $AAOD = (1 - SSA) * AOD$). Figure 7 also shows that the
784 AERONET Level-2 SSA values are similar to the monthly in-situ and AeroCom SSA medians
785 between April and November. There are no AERONET Level-2 almucantar retrievals of SSA in
786 January or December at either site. For the remaining months, median Level-2 almucantar
787 retrievals of SSA are based on very few data points resulting in bigger discrepancies between
788 AERONET Level-2 almucantar retrievals of SSA and the in-situ and AeroCom SSA values.

789

790 Aside from differences in magnitude, there are also differences in the seasonal patterns of AOD,
791 AAOD and SSA for the three data sets (in-situ, AERONET 1.5* and AeroCom). For example, at
792 BND, the AERONET and in-situ AAOD both have a bi-modal annual distribution with peaks in
793 late spring and early fall, which is not captured by the AeroCom AAOD and which is not seen in
794 the AOD seasonality. The observed seasonal differences may be a result of (a) the different
795 climatology time ranges for each method and/or (b) very little overlap in the measurement times
796 for AERONET and in-situ measurements or (c) in the case of the models, not capturing local
797 emissions near the sites. This highlights the importance of direct (i.e., near in time and space)
798 comparisons in order to understand these seasonal differences. The seasonal cycle plots in
799 Figure 7 also direct attention to the fact that AOD and AAOD vary independently rather than
800 exhibiting the same seasonal pattern. This suggests that different emission sources and/or
801 atmospheric processes control the variability of absorption and scattering aerosol over the
802 course of the year.

803

804 3.4 Discussion

805 Because AERONET data are readily available and are being widely used as a benchmark data
806 set for evaluating model output of AAOD (e.g., Chung et al., 2012; Bond et al., 2013; He et al.,
807 2014; Wang et al., 2014) as well as for comparison with satellite retrievals and development of
808 AAOD climatologies, we document and discuss some of the previous methods for utilizing
809 existing AERONET retrievals that have been used to minimize the bias in retrieved AAOD at low
810 AOD. These approaches fall into several categories (1) use only Level-2 data; (2) use Level-2
811 and Level-1.5 data with acknowledgement of greater uncertainty in the retrievals and potentially
812 additional measurement constraints for the Level-1.5 data; (3) make climatological assumptions
813 about the representativeness of Level-2 SSA for low AOD conditions to obtain AAOD.

814 Clearly the simplest approach to minimize bias in retrieved AAOD and SSA is to only use
815 AERONET Level-2 retrievals as those have the lowest uncertainty. This approach has been and



816 continues to be used (e.g., Koch et al., 2009; Bahadur et al., 2010; Chung et al., 2012; Buchard
817 et al., 2015; Pan et al., 2015; Li et al., 2015). However, as shown in Figure 1 the vast majority
818 of the globe has $AOD_{440} < 0.4$, meaning few if any AERONET Level-2 AAOD or SSA retrievals
819 will be available for most locations. This approach is quite useful in regions (or for case studies)
820 with high aerosol loading (high AOD). However, removing low absorption events will cause
821 AAOD statistics to be biased high.

822 Some studies have utilized AERONET Level-1.5 retrievals of absorption-related aerosol
823 properties in order to avoid the high AOD levels required by Level-2 data (e.g., Lacagnina et al.,
824 2015; Mallet et al., 2013). These studies note that Level-1.5 data include more relevant AOD
825 values but that there are accompanying higher uncertainties in the retrievals for absorption
826 related properties. Mallet et al. (2013) use Level-1.5 data to evaluate the spectral dependence
827 of aerosol absorption. Lacagnina et al. (2015) utilize both Level-2 and Level-1.5 AERONET data
828 in their comparison with PARASOL satellite retrievals of SSA and AAOD. For the Level-1.5
829 data they apply the additional requirement that the solar zenith angle must be $\geq 50^\circ$. Lacagnina
830 et al. (2015) find quite good agreement (within ± 0.03) for AAOD and note that larger
831 differences between PARASOL and AERONET retrieval occur at higher AOD conditions,
832 possibly due to less homogenous aerosol (i.e., plumes).

833 A more sophisticated approach to deal with SSA (and hence AAOD uncertainties) at low AOD is
834 implemented by Wang et al. (2014). They make the assumption that SSA is independent of
835 AOD (at least as a function of season) and utilize climatological Level-2 SSA values for each
836 season with the measured AOD in order to obtain AAOD. The seasonal climatologies of SSA
837 are based on 12 years of Level-2 AERONET data. For the two US continental sites studied in
838 this paper, the approach of Wang et al. (2014) would likely minimize the potential AERONET
839 bias towards high AAOD at low AOD conditions as the Level-2 monthly climatological SSA
840 values are quite similar to SSA values obtained by in-situ measurements (Fig. 7).

841 A similar, though statistical, approach was used in Bond et al.'s (2013) bounding BC paper in
842 order to reduce the uncertainty in AERONET SSA retrievals at low AOD. Bond et al. (2013)
843 worked with monthly local statistics of at least 10 inversion samples. After recovering SSA data
844 from the lower quality Level-1.5 into the Level-2 data (AERONET Level-1.5*), the SSA value
845 corresponding to AOD_{550} of 0.25 was prescribed for all observations at lower AOD, while for
846 locations with all $AOD_{550} < 0.25$, the average SSA of the upper 20th percentile of AOD
847 observations was prescribed for all lower AOD.

848 One drawback affecting approaches using climatological values of SSA (e.g., Wang et al., 2014;
849 Bond et al., 2013) is that they may not account for the systematic variability that has been
850 observed between SSA and loading at many sites, although AOD is usually more variable than
851 the composition (or SSA). Still some studies with in-situ data (e.g., Delene and Ogren, 2002;
852 Andrews et al., 2013; Pandolfi et al., 2014; Sherman et al., 2015) indicate that SSA
853 systematically decreases with decreasing aerosol loading. A similar SSA/AOD systematic
854 variability relationship is also observed at some North American AERONET sites. Schafer et al.
855 (2014; their figure 6) shows SSA decreasing at lower loading for the GSFC site near
856 Washington D.C. during the period of their field campaign; they also show similar relationships



857 between SSA and AOD based on the long-term data for three mid-Atlantic AERONET sites.
858 Additionally, a quick survey (not shown) of other long-term North American AERONET sites with
859 good statistics (i.e., lots of points) for Level-1.5 SSA retrievals (e.g., Billerica (Massachusetts),
860 Bratts Lake (Saskatchewan, Canada), COVE (Virginia), Egbert (Ontario, Canada), Fresno
861 (California), Konza (Kansas), SERC (Maryland), and University of Houston (Texas)) indicates
862 this systematic relationship may be observed at a wide range of locations in North America.
863 Such climatological analyses may mask short-lived and/or infrequent aerosol events (e.g., dust
864 or smoke incursions) that may have significantly different optical properties.

865 Figure 8 shows the systematic relationships between SSA_{440} and AOD_{440} for BND and SGP for
866 both the AERONET retrievals and in-situ profile measurements. Consistent with previous
867 figures, we have utilized SSA values for $AOD_{440} < 0.4$ when there was a valid Level-2 AOD
868 inversion retrieval, i.e., what we call AERONET Level-1.5*. Also included on the figure is a line
869 showing the SSA_{550} versus scattering ($\sigma_{sp,550}$) relationships for the surface measurements at
870 BND and SGP. The surface measurements are for low RH conditions ($RH < 40\%$); adjustment of
871 the surface measurements to ambient conditions would tend to shift the SSA_{550} values upward
872 (assuming absorption is not affected) and the scattering values to the right, but would not
873 significantly change the shape of the curve.

874
875 Figure 8 suggests that for all three sets of measurements at both sites, there is a consistent
876 decrease in SSA as aerosol loading decreases. The AERONET SSA values are lower than the
877 in-situ profile values as would be expected from the results presented in sections 3.1 and 3.3.
878 At the lowest AOD values ($AOD_{440} \sim 0.05$) the AERONET SSA values diverge, consistent with
879 very large uncertainties expected in the AERONET SSA retrievals in the cleanest conditions.
880 Uncertainty in the AERONET AOD retrieval may begin to affect the AERONET SSA retrieval
881 where ± 0.01 AOD uncertainty is equivalent to a 20% change in AOD for AOD of 0.05. In
882 addition, at such low AOD values, the surface reflectance uncertainties may influence
883 AERONET's retrieval of SSA. Figure 8 suggests that, in terms of the shape of the systematic
884 variability plot, there are no obvious retrieval issues for AERONET SSA retrievals in the range
885 $0.05 < AOD_{440} < 0.2$, although this is in the AOD range where high uncertainty in the SSA retrieval
886 is expected (Dubovik et al., 2000).

887
888 There are large differences (orders of magnitude) in the number of data points in each of the
889 data sets; the number of points in each bin is indicated by the color-coded histograms shown on
890 Figure 8. The mean standard error (MSE) in SSA ($MSE = (\text{standard deviation}) / (\text{number of}$
891 $\text{points})^{1/2}$) is indicated by the shading surrounding the solid colored lines. The MSE is quite
892 similar for the AERONET 1.5* and in-situ profile measurements across the AOD range plotted in
893 Figure 8, suggesting the observed systematic variability is not merely due to small numbers of
894 data points in each bin, particularly at lower loading. However, the fact that the AERONET MSE
895 is approximately the same as the in-situ profile MSE, despite having approximately an order of
896 magnitude larger number of points/bin, indicates that variability in the retrieved AERONET SSA
897 is larger than the variability in SSA derived from in-situ profile measurements.

898 This study has utilized a valuable but spatially limited (i.e., two rural continental North American
899 sites) climatological vertical profile dataset to explore AERONET retrievals of AAOD. Clearly,



900 one way to address the observed bias in AAOD is to pursue a focused measurement program
901 designed to acquire statistically robust in-situ vertical profiles over AERONET sites representing
902 a wide range of conditions and aerosol types. This type of measurement program is being
903 considered at NASA to evaluate satellite retrievals and better characterize atmospheric aerosol
904 (R. Kahn, SAM-CAAM, pers. comm.). Additional evaluation of the AERONET retrieval algorithm
905 may also provide insight into a potential SSA and, thus, AAOD bias (e.g., Hashimoto et al.,
906 2012). While an AERONET bias towards high AAOD will affect global radiative forcing
907 estimates if models upscale their simulated absorption to match the AERONET retrievals, the
908 work of Wang et al. (2016) has shown that other factors (e.g., the spatial resolution of models
909 and emissions) may also contribute to the differences observed between model and AERONET
910 retrievals of AAOD. Thus, to really be able to understand and simulate the influence of
911 absorbing aerosol on radiative forcing will require expanded effort on both the measurement
912 and modeling fronts.

913

914 4. Conclusion

915 We cannot say how to estimate SSA or AAOD from AERONET retrievals for the low AOD
916 conditions prevalent around much of the globe. AERONET retrievals of SSA at low AOD
917 conditions appear to be biased low and to over-predict absorbing aerosol relative to coincident
918 and co-located in-situ vertical profile measurements. This suggests that scaling modelled black
919 carbon concentrations upwards to match AERONET retrievals of AAOD may lead to aerosol
920 absorption overestimates in regions of low AOD. The magnitude of this bias is unknown and
921 may be close to or within the uncertainty estimates for the retrievals. If the discrepancy between
922 the in-situ and AERONET AAOD is due to issues with the in-situ measurements of absorption,
923 the only way we see to increase the in-situ absorption values is a significant enhancement (on
924 the order of factor of 2 or more) in absorption due to a coating effect.

925 Some in-situ measurements suggest that a systematic relationship exists between SSA and
926 AOD, but these measurements are spatially sparse and typically not made at ambient
927 conditions. Nonetheless, systematic relationships between SSA and AOD, similar to those seen
928 in the in-situ data at the two sites, are also observed for multiple North American AERONET
929 sites. The existence of such a systematic relationship may limit the accuracy of AAOD
930 estimates when climatological values for SSA are assumed for low loading conditions.
931 However, the use of statistically-based values of SSA (i.e., local or regional SSA values derived
932 for higher AOD conditions) to retrieve AAOD at lower AOD will at least avoid a high bias for
933 AAOD, as would occur when absorption at low AOD ($AOD_{440} < 0.4$) is not considered (as is the
934 case for AERONET Level-2.0 data).

935

936 **Acknowledgements**

937 Funding for the SGP airplane measurements was provided by DOE/ARM, while the BND
938 airplane measurements were funded by NOAA's Climate Program Office. Greenwood Aviation
939 and FlightSTAR provided fabulous pilots and maintenance of the aircraft. Derek Hageman



940 (University of Colorado) is owed much for his coding genius and Patrick Sheridan
941 (NOAA/ESRL/GMD) for making instruments on both airplanes work and ensuring the quality of
942 the BND aircraft data set. We thank the modelling groups for providing AeroCom Phase II
943 results. We greatly appreciate the ease of access to and use of IMPROVE aerosol chemistry
944 data for the Bondville and Cherokee Nation IMPROVE sites. IMPROVE data were downloaded
945 from: <http://views.cira.colostate.edu/web/DataWizard/>. This study was supported by NOAA
946 Climate Program Office's Atmospheric Chemistry, Carbon Cycle and Climate (AC4) program.
947 BHS acknowledges funding by the Research Council of Norway through the grants AC/BC
948 (240372) and NetBC (244141). We also gratefully acknowledge the very helpful discussions
949 from David Giles and Brent Holben from AERONET.

950

951

952 **References**

- 953 Adam M., Putaud, J.P., Martins dos Santos, S., Dell'Acqua, A., Gruening, C., "Aerosol
954 hygroscopicity at a regional background site (Ispra) in Northern Italy," *Atmos. Chem. Phys.*,
955 12, 5703–5717, 2012.
- 956 Anderson, T. L., Charlson, R. J., Winker, D. M., Ogren, J. A., and Holmén, K., "Mesoscale
957 Variations of Tropospheric Aerosols," *J. Atmos. Sci.*, 60, 119–136, 2003.
- 958 Anderson, T. L. and Ogren, J. A., "Determining aerosol radiative properties using the TSI 3563
959 integrating nephelometer," *Aerosol Sci. Technol.*, 29, 57–69, 1998.
- 960 Andrews, E., Sheridan, P.J., Ogren, J.A., "Seasonal Differences in the Vertical Profiles of
961 Aerosol Optical Properties over Rural Oklahoma," *Atmos. Chem. Phys.*, 11, 10661–10676,
962 2011a.
- 963 Andrews, E., et al. "Climatology of aerosol radiative properties in the free troposphere," *Atmos.*
964 *Res.*, 102, 365-393, 2011b.
- 965 Arnott, W.P., Hamasha, K., Moosmuller, H., Sheridan, P.J., Ogren, J.A., "Towards aerosol light-
966 absorption measurements with a 7-wavelength aethalometer: evaluation with a
967 photoacoustic instrument and 3-wavelength Nephelometer," *Aerosol Sci. Technol.*, 39, 17-29,
968 2005.
- 969 Bahadur, R., Praveen, P. S., Xu, Y., and Ramanathan, V., "Solar absorption by elemental and
970 brown carbon determined from spectral observations," *P. Natl. Acad. Sci. USA*, 109, 43,
971 17366–17371, doi:10.1073/pnas.1205910109, 2012.
- 972 Bond, T. C., Anderson, T. L., and Campbell, D., "Calibration and intercomparison of filter-based
973 measurements of visible light absorption by aerosols," *Aerosol Sci. Technol.*, 30, 582–600,
974 doi:10.1080/027868299304435, 1999.
- 975 Bond, T. C., et al., "Bounding the role of black carbon in the climate system: A scientific
976 assessment," *J. Geophys. Res.*, 118, 5380–5552, doi:10.1002/jgrd.50171, 2013.
- 977 Bond, T. C., Habib, G., Bergstrom, R.W., "Limitations in the enhancement of visible light
978 absorption due to mixing state," *J. Geophys. Res.*, 111, D20211, doi:10.1029/2006JD007315,
979 2006.
- 980 Brem, B.T., Mena Gonzalez, F.C., Meyers, S.R., Bond, T.C., Rood, M.J., "Laboratory-Measured
981 Optical Properties of Inorganic and Organic Aerosols at Relative Humidities up to 95%,"
982 *Aerosol Sci. Technol.*, 46:2, 178-190, 2012.
- 983 Buchard, V. da Silva, A.M., Colarco, P.R., Darmenov, A., Randles, C.A., Govindaraju, R.,
984 Torres, O., Campbell, J., Spurr, R. "Using the OMI aerosol index and absorption aerosol
985 optical depth to evaluate the NASA MERRA Aerosol Reanalysis," *Atmos. Chem. Phys.*, 15,
986 5743–5760, 2015.
- 987 Burrows, J. P., Dehn, A., Deters, B., Himmelman, S., Richter, A., Voigt, S. and Orphal, J.,
988 "Atmospheric Remote-Sensing Reference Data from GOME: Part 1. Temperature-



- 989 Dependent Absorption Cross-sections of NO₂ in the 231-794 nm Range,” *JQSRT*, 60, 1025-
990 1031, 1998.
- 991 Carrico, C.M., Kus, P., Rood, M.J., Quinn, P.K., Bates, T.S., “Mixtures of pollution, dust, sea salt
992 and volcanic aerosol during ACE-Asia: Radiative properties as a function of relative
993 humidity,” *J. Geophys. Res.*, 108, doi:10.1029/2003JD003405, 2003.
- 994 Cappa, C.D., et al., “Radiative absorption enhancements due to the mixing state of atmospheric
995 black carbon,” *Science*, 337, 1078-1081, 2012.
- 996 Chin, M., T. Diehl, T., Dubovik, O., Eck, T.F., Holben, B.N., Sinyuk, A., Streets, D.G., “Light
997 absorption by pollution, dust, and biomass burning aerosols: a global model study and
998 evaluation with AERONET measurements,” *Ann. Geophys.*, 27, 3439-3464, 2009.
- 999 Corr, C.A., Krotkov, N., Madronich, S., Slusser, J.R., Holben, B., Gao, W., Flynn, J., Lefer, B.,
1000 Kreidenweis, S.M., “Retrieval of aerosol single scattering albedo at ultraviolet wavelengths at
1001 the T1 site during MILAGRO,” *Atmos. Chem. Phys.*, 9, 5813-5827, 2009.
- 1002 Corrigan, C.E., Roberts, G.C., Ramana, M.V., Kim, D., Ramanathan, V., “Capturing vertical
1003 profiles of aerosols and black carbon over the Indian Ocean using autonomous unmanned
1004 vehicles,” *Atmos. Chem Phys*, 8, 737-747, 2009.
- 1005 Crumeyrolle, S., Chen, G., Ziemba, L., Beyersdorf, A., Thornhill, L., Winstead, E., Moore, R.,
1006 Shook, M.A., Anderson, B., “Factors that influence surface PM_{2.5} values inferred from
1007 satellite observations: perspective gained for the Baltimore-Washington Area during
1008 DISCOVER-AQ,” *Atmos. Chem. Phys.*, 14, 2139-2153, 2014.
- 1009 Delene, D. J. and Ogren, J. A., “Variability of aerosol optical properties at four North American
1010 surface monitoring sites,” *J. Atmos. Sci.*, 59, 1135–1150, 2002.
- 1011 Doran, J.C., Barnard, J.C., Arnott, W.P., Cary, R., Coulter, R., Fast, J.D., Kassianov, E.I.,
1012 Kleinman, L., Laulainen, N.S., Martin, T., Paredes-Miranda, G., Pekour, M.S., Shaw, W.J.,
1013 Smith, D.F., Springston, S.R., Yu, X.-Y., “The T1-T2 study: evolution of aerosol properties
1014 downwind of Mexico City,” *Atmos. Chem. Phys.*, 7, 1585-1598, 2007.
- 1015 Dubovik, O. and King, M.D., “A flexible inversion algorithm for retrieval of aerosol optical
1016 properties from Sun and sky radiance measurements,” *J. Geophys. Res.*, 105, 20673-20696,
1017 2000.
- 1018 Dubovik, O., Sinyuk, A., Lapyonok, T., Holben, B. N., Mishchenko, M., Yang, P., Eck, T. F.,
1019 Volten, H., Munoz, O., Veihelmann, B., van der Zande, W.J., Leon, J.-F., Sorokin, M.,
1020 Slutsker, I., “Application of spheroid models to account for aerosol particle nonsphericity in
1021 remote sensing of desert dust,” *J. Geophys. Res.*, 111, doi:10.1029/2005JD006619, 2006.
- 1022 Dubovik, O., A. Smirnov, B.N. Holben, M.D. King, Y. J. Kaufman, T.F. Eck and I. Slutsker,
1023 “Accuracy assessment of aerosol optical properties retrieval from AERONET sun and sky
1024 radiance measurements,” *J. Geophys. Res.*, 105, 9791-9806, 2000.
- 1025 Eck, T.F., Holben, B.N., Reid, J.S., Dubovik, O., Smirnov, A., O'Neill, N.T., Slutsker, I. Kinne, S.,
1026 “Wavelength dependence of the optical depth of biomass burning, urban and desert dust
1027 aerosols,” *J. Geophys. Res.*, 104, 31 333-31 350, 1999.
- 1028 Esteve, A.R., Ogren, J.A., Sheridan, P.J., Andrews, E., Holben, B.N., and Utrillas, M.P.,
1029 “Statistical evaluation of aerosol retrievals from AERONET using in-situ aircraft
1030 measurements,” *Atmos. Chem. Phys.*, 12, 2987-3003, 2012.
- 1031 Ferrero, L., Mocnik, G., Ferrini, B.S., Perrone, M.G., Sangiorgi, G., Bolzacchini, E., “Vertical
1032 profiles of aerosol absorption coefficient from micro-aethalometer data and Mie calculation
1033 over Milan,” *Sci. Tot. Environ*, 409, 2824-2837, 2011.
- 1034 Formenti, P., et al., “STAAARTE-MED 1998 summer airborne measurements over the Aegean
1035 Sea, 2, Aerosol scattering and absorption, and radiative calculations,” *J. Geophys. Res.*,
1036 107(D21), 4451, doi:10.1029/2001JD001536, 2002.
- 1037 Giles, D.M., Holben, B.N., Eck, T.F., Sinyuk, A., Smirnov, A., Slutsker, I., Dickerson, R.R.,
1038 Thompson, A.M., Schafer, J.S., “An analysis of AERONET aerosol absorption properties and



- 1039 classifications representative of aerosol source region," *J. Geophys. Res.*, 117, doi:
 1040 10.1029/2012JD018127, 2012.
- 1041 Hamonou, E., Chazette, P., Balis, D., Schneider, X., Galani, E., Ancellet, G., Papayannis, A.,
 1042 "Characterization of the vertical structure of Saharan dust export to the Mediterranean basin,"
 1043 *J. Geophys. Res.*, 104, 22257-22270, 1999.
- 1044 Hänel, G., "The properties of atmospheric aerosol particles as functions of the relative humidity
 1045 at thermodynamic equilibrium with surrounding moist air," *Adv. Geophys.*, 73-188, 1976.
- 1046 Hansen, J., Sato, M., Ruedy, R., "Radiative forcing and climate response," *J. Geophys. Res.*,
 1047 102, 6831-6864, 1997.
- 1048 Hartley, W.S., Hobbs, P.V., Ross, J.L., Russell, P.B., Livingston, J.M., "Properties of aerosols
 1049 aloft relevant to direct aerosol radiative forcing off the mid-Atlantic coast of the United
 1050 States," *J. Geophys. Res.*, 105, 9859-9885, 2000.
- 1051 Haywood, J.M., P. Francis, O. Dubovik, M. Glew, and B. Holben, Comparison of aerosol size
 1052 distributions, radiative properties, and optical depths determined by aircraft observations and
 1053 Sun photometers during SAFARI 2000, *J. Geophys. Res.*, 108(D13), 8471,
 1054 doi:10.1029/2002JD002250, 2003.
- 1055 Haywood, J.M. and Ramaswamy, V., "Global sensitivity studies of the direct radiative forcing due
 1056 to anthropogenic sulfate and black carbon aerosols," *J. Geophys. Res.*, 103, 6043-6058,
 1057 1998.
- 1058 Haywood, J.M. and Shine, K.P., "The effect of anthropogenic sulfate and soot aerosol on the
 1059 clear sky planetary radiation budget," *Geophys. Res. Lett.*, 22, 603-606, 1995.
- 1060 Hinds, W.C., *Aerosol Technology: Properties, behavior and measurement of airborne particles*,
 1061 John Wiley and Sons, New York, 1982.
- 1062 Holben, B. N., et al., "AERONET—A federated instrument network and data archive for aerosol
 1063 characterization," *Remote Sens. Environ.*, 66, 1–16, 1998.
- 1064 Holben, B.N., Eck, T.F., Slutsker, I., Smirnov, A., Sinyuk, A., Schafer, J., Giles, D., Dubovik O.,
 1065 "AERONET's Version 2.0 quality assurance criteria,"
 1066 http://aeronet.gsfc.nasa.gov/new_web/Documents/AERONETcriteria_final1.pdf, 2006.
- 1067 Johnson, B.T., Christopher, S., Haywood, J.M., Osborne, S.R., McFarlane, S., Hsu, C.,
 1068 Salustro, C., Kahn, R., "Measurements of aerosol properties from aircraft, satellite and
 1069 ground-based remote sensing: A case-study from the Dust and Biomass-burning Experiment
 1070 (DABEX)," *Q. J. R. Meteorol. Soc.*, 135, 922–934, 2009.
- 1071 Johnson, B.T., Osborne, S.R., "Physical and optical properties of mineral dust aerosol
 1072 measured by aircraft during the GERBILS campaign," *Q.J.R.Meteorol. Soc.*, 137, 1117-1130,
 1073 2011.
- 1074 Kasten, F., "Visibility forecast in the phase of pre-condensation," *Tellus*, 21, 631-635, 1969.
- 1075 Kelektsoylou, K., Rapsomanikis, S., Karageorgos, E.T., Kosmadakis, I., Optical properties of
 1076 aerosol over a Southern European urban environment," *Int.J. Remote Sens.*, 33, 1214-1233,
 1077 2012.
- 1078 Kinne et al., "An AeroCom initial assessment – optical properties in aerosol component modules
 1079 of global models," *Atmos. Chem. Phys.*, 6, 1–20, 2006.
- 1080 Koch, D., et al., "Evaluation of black carbon estimations in global aerosol models," *Atmos.Chem.*
 1081 *Phys.*, 9, 9001–9026, doi:10.5194/acp-9-9001-2009, 2009.
- 1082 Kotchenruther, R. A., Hobbs, P.V., Hegg, D.A., "Humidification factors for atmospheric aerosols
 1083 off the mid-Atlantic coast of the United States," *J. Geophys. Res.*, 104, 2239– 2251, 1999.
- 1084 Lacagnina, C., Hasekamp, O.P., Bian, H., Curci, G., Myhre, G., van Noije, T, Schulz, M., Skeie,
 1085 R.B., Takemura, T., Zhang, K., "Aerosol single-scattering albedo over the global oceans:
 1086 Comparing PARASOL retrievals with AERONET, OMI, and AeroCom models estimates," *J.*
 1087 *Geophys. Res. Atmos.*, 120, 9814–9836, doi:10.1002/2015JD023501, 2015.



- 1088 Lack, D.A., et al., "Relative humidity dependence of light absorption by mineral dust after long-
1089 range atmospheric transport from the Sahara," *Geophys. Res. Lett.*, 36, L24805,
1090 doi:10.1029/2009GL041002, 2009.
- 1091 Lack, D.A., Richardson, M.S., Law, D., Langridge, J.M., Cappa, C.D., McLaughlin, R.J., and
1092 Murphy, D.M.: Aircraft Instrument for Comprehensive Characterization of Aerosol Optical
1093 Properties, Part 2: Black and Brown Carbon Absorption and Absorption Enhancement
1094 Measured with Photo Acoustic Spectroscopy, *Aerosol Sci. Tech.*, 46:5, 555-568, DOI:
1095 10.1080/02786826.2011.645955, 2012.
- 1096 Leahy, L.V., Anderson, T.L., Eck, T.F., Bergstrom, R.W., "A synthesis of single scattering
1097 albedo of biomass burning aerosol over southern Africa during SAFARI 2000," *Geophys.*
1098 *Res. Lett.*, 34, doi:10.1029/2007GL029697, 2007.
- 1099 Li, S., Kahn, R., Chin, M., Garay, M.J., Liu, Y., "Improving satellite-retrieved aerosol
1100 microphysical properties using GOCART data," *Atmos. Meas. Tech.*, 8, 1157–1171, 2015.
- 1101 Magi, B.I., Hobbs, P.V., Kirchstetter, T.W., Novakov, T., Hegg, D.A., Gao, S., Redemann, J.,
1102 Schmid, B., "Aerosol Properties and Chemical Apportionment of Aerosol Optical Depth at
1103 Locations off the U.S. East Coast in July and August 2001," *J. Atmos. Sci.*, 62, 919-933,
1104 2005.
- 1105 Mallet, M., Dubovik, O., Nabat, P., Dulac, F., Kahn, R., Sciare, J., Paronis, D., and Léon, J. F.,
1106 "Absorption properties of Mediterranean aerosols obtained from multi-year, ground-based
1107 remote sensing observations," *Atmos. Chem. Phys.*, 13, 9195-9210, 2013.
- 1108 Mallet, M., Van Dingenen, R., Roger, J. C., Despiiau, S., Cachier, H., "In situ airborne
1109 measurements of aerosol optical properties during photochemical pollution events," *J.*
1110 *Geophys. Res.*, 110, D03205, doi:10.1029/2004JD005139, 2005.
- 1111 Mallet, M., Pont, V., Liousse, C., Gomes, L., Pelon, J., Osborne, S., Haywood, J., Roger, J.C.,
1112 Dubuisson, P., Mariscal, A., Thouret, V., Gouloub, P., "Aerosol direct radiative forcing of
1113 Djougou (northern Benin) during the African Monsoon Multidisciplinary, Analysis dry season
1114 experiment (special observation period – 0)," *J. Geophys. Res.*, 113,
1115 doi:1029/2007JD009419, 2008.
- 1116 Malm, W.C., Sisler, J.F., Huffman, D., Eldred, R.A., Cahill, T.A., "Spatial and seasonal trends in
1117 particle concentration and optical extinction in the United States," *J. Geophys. Res.* 99,
1118 1347–1370, 1994.
- 1119 McConnell, C.L., Highwood, E.J., Coe, H., Formenti, P., Anderson, B., Osborne, S., Nava, S.
1120 Desboeufs, K., Chen, G., and Harrison, M.A.J., "Seasonal variations of the physical and
1121 optical characteristics of Saharan dust: Results from the Dust Outflow and Deposition to the
1122 Ocean (DODO) experiment," *J. Geophys. Res.*, 113, doi:10.1029/2007JD009606, 2008.
- 1123 McMeeking, G. R., Fortner, E., Onasch, T.B., Taylor, J.W., Flynn, M., Coe, H., Kreidenweis,
1124 S.M. "Impacts of nonrefractory material on light absorption by aerosols emitted from biomass
1125 burning," *J. Geophys. Res. Atmos.*, 119, 12,272–12,286, doi:10.1002/2014JD021750, 2014.
- 1126 Müller, D. Lee, K.-H., Gasteiger, J., Tesche, M., Weinzierl, B., Kandler, K., Müller, T., Toledano,
1127 C., Otto, S., Althausen, D., Ansmann, A., "Comparison of optical and microphysical
1128 properties of pure Saharan mineral dust observed with AERONET Sun photometer, Raman
1129 lidar, and in situ instruments during SAMUM 2006," *J. Geophys. Res.*, 117, doi:
1130 10.1029/2011JD016825, 2012.
- 1131 Müller, T., et al. "Characterization and intercomparison of aerosol absorption photometers:
1132 result of two intercomparison workshops" *Atmos. Meas. Tech.*, 4, 245–268, 2011.
- 1133 Myhre G., Samset, B.H., Schulz, M. et al., "Radiative forcing of the direct aerosol effect from
1134 AeroCom Phase II simulations," *Atmos. Chem. Phys.*, 13, 1853–1877, 2013
- 1135 Nessler, R., Weingartner, E., Baltensperger, U., "Effect of humidity on aerosol light absorption
1136 and its implications for extinction and the single scattering albedo illustrated for a site in the
1137 lower free troposphere," *J. Aerosol Sci.*, 36, 958–972, 2005.



- 1138 Ogren, J. A., "Comment on "Calibration and Intercomparison of Filter-Based Measurements of
1139 Visible Light Absorption by Aerosols", Aerosol Sci. Technol., 44, 589–591,
1140 doi:10.1080/02786826.2010.482111, 2010.
- 1141 O'Neill, N. T., Eck, T. F., Smirnov, A., Holben, B. N., Thulasiraman, S., "Spectral discrimination
1142 of coarse and fine mode optical depth," J. Geophys. Res., 108, 4559-4573, 2003.
- 1143 Osborne, S. R., Johnson, B. T., Haywood, J. M., Baran, A. J., Harrison, M. A. J., McConnell,
1144 C.L., "Physical and optical properties of mineral dust aerosol during the Dust and Biomass-
1145 burning Experiment, J. Geophys. Res., 113, D00C03, doi:10.1029/2007JD009551, 2008.
- 1146 Pan, X., Chin, M., Gautam, R., Bian, H., Kim, D., Colarco, P.R., Diehl, T.L., Takemura, T.,
1147 Pozzoli, L., Tsigaridis, K., Bauer, S., Bellouin, N., "A multi-model evaluation of aerosols over
1148 South Asia: common problems and possible causes," Atmos. Chem. Phys., 15, 5903–5928,
1149 2015.
- 1150 Parworth, C., Fast, J., Meib, F., Shipper, T., Sivaraman, C., Tilp, A., Watson, T., Zhang, Q.,
1151 "Long-term measurements of submicrometer aerosol chemistry at the Southern Great Plains
1152 (SGP) using an Aerosol Chemical Speciation Monitor (ACSM)," Atmos. Environ., 106, 43–55,
1153 2015.
- 1154 Petzold, A., Ogren, J.A., Fiebig, M., Laj, P., Li, S.-M., Baltensperger, U., Holzer-Popp, T., Kinne,
1155 S., Pappalardo, G., Sugimoto, N., Wehrli, C., Wiedensohler, A., Zhang, X.-Y.,
1156 "Recommendations for reporting "black carbon" measurements," Atmos. Chem. Phys., 13,
1157 8365-8379, 2013.
- 1158 Quinn, P.K., Bates, T.S., Baynard, T., Clarke, A.D., Onasch, T.B., Wang, W., Rood, M.J.,
1159 Andrews, E., Allan, J., Carrico, C.M., Coffman, D., Worsnop, D., "Impact of particulate
1160 organic matter on the relative humidity dependence of light scattering: A simplified
1161 parameterization," Geophys. Res. Lett., 32, doi:10.1029/2005GL024322, 2005.
- 1162 Ramanathan, V., Carmichael, G., "Global and regional climate changes due to black carbon,"
1163 Nature – Geosci., 1(4), 221-227, 2008.
- 1164 Reddy, M. S., Boucher, O., Bellouin, N., Schulz, M., Balkanski, Y., Dufresne, J.L., Pham, M.,
1165 "Estimates of global multicomponent aerosol optical depth and direct radiative perturbation in
1166 the Laboratoire de Meteorologie Dynamique general circulation model," J. Geophys. Res.,
1167 110, doi:10.1029/2004jd004757, 2005.
- 1168 Redemann, J., Russell, P.B., Hamill, P., "Dependence of aerosol light absorption and single
1169 scattering albedo on ambient relative humidity for sulfate aerosols with black carbon cores,"
1170 J. Geophys. Res., 106, 27485-27495, 2001.
- 1171 Reid, J.S., Hobbs, P.V., Liousse, C., Vanderlei Martins, J., Weiss, R.E., Eck, T.F.,
1172 "Comparisons of techniques for measuring shortwave absorption and black carbon content of
1173 aerosols from biomass burning in Brazil," J. Geophys. Res., 103, 32031-32040, 1998.
- 1174 Samset, B.H. et al., "Black carbon vertical profiles strongly affect its radiative forcing
1175 uncertainty," Atmos. Chem. Phys., 13, 2423–2434, 2013.
- 1176 Sato, M., Hansen, J., Kock, D., Lacis, A., Ruedy, R., Dubovik, O., Holben, B., Chin, M.,
1177 Novakov, T., "Global atmospheric black carbon inferred from AERONET," PNAS, 100, 6319-
1178 6324, 2003.
- 1179 Schafer, J.S., Eck, T.F., Holben, B.N., Thornhill, K.L., Anderson, B.E., Sinyuk, A., Giles, D.M.,
1180 Winstead, E.L., Ziemba, L.D., Beyersdorf, A.J., Kenny, P.R., Smirnov, A., Slutsker, I.,
1181 "Intercomparison of aerosol single-scattering albedo derived from AERONET surface
1182 radiometers and LARGE in situ aircraft profiles during the 2011 DRAGON-MD and
1183 DISCOVER-AQ experiments," J. Geophys. Res., 119, 7439–7452,
1184 doi:10.1002/2013JD021166, 2014.
- 1185 Schmid, B., Flynn, C.J., Newsom, R.K., Turner, D.D., Ferrare, R.A., Clayton, M.F., Andrews, E.,
1186 Ogren, J.A., Johnson, R.R., Russell, P.B., Gore, W.J., Dominguez, R., "Validation of aerosol
1187 extinction and water vapor profiles from routine Atmospheric Radiation Measurement



- 1188 Program Climate Research Facility measurements," *J. Geophys. Res.*, 114,
1189 doi:10.1029/2009JD012682, 2009.
- 1190 Schwarz, J.P., Spackman, J.R., Fahey, D.W., Gao, R.W., Lohmann, U., Stier, P., Watts, L.A.,
1191 Thomson, D.S., Lack, D.A., Pfister, L., Mahoney, M.J., Baumgardner, D., Wilson, J.C.,
1192 Reeves, J.M., "Coatings and their enhancement of black carbon light absorption in the
1193 tropical atmosphere," *J. Geophys. Res.*, 113, D03203, doi:10.1029/2007JD009042, 2008.
- 1194 Schwarz, J.P., Spackman, J.R., Gao, R.S., Watts, L.A., Stier, P., Schulz, M., Davis, S.M.,
1195 Wofsy, S.C., Fahey, D.W., "Global-scale black carbon profiles observed in the remote
1196 atmosphere and compared to models," *Geophys. Res. Lett.*, 27, doi:10.1029/2010GL044372,
1197 2010.
- 1198 Sharma, S., Ishizawa, M., Chan, D., Lavoue, D., Andrews, E., Eleftheriadis, K., Maksyutov, S.,
1199 "16-year simulation of Arctic black carbon: transport, source contribution, and sensitivity
1200 analysis on deposition," *J. Geophys. Res.* 118, 1–22, doi:10.1029/2012JD017774, 2013.
- 1201 Sheridan, P. J., Andrews, E., Ogren, J. A., Tackett, J. L., and Winker, D. M.: Vertical profiles of
1202 aerosol optical properties over Central Illinois and comparison with surface and satellite
1203 measurements, *Atmos. Chem. Phys.*, 12, 11695–11721, 2012.
- 1204 Sheridan, P. J., Arnott, W. P., Ogren, J. A., Andrews, E., Atkinson, D. B., Covert, D. S.,
1205 Moosmüller, H., Petzold, A., Schmid, B., Strawa, A. W., Varma, R., and Virkkula, A.: The
1206 Reno Aerosol Optics Study: An Evaluation of Aerosol Absorption Measurement Methods,
1207 *Aerosol Sci. Tech.*, 39, 1–16, 2005.
- 1208 Sheridan, P. J., Delene, D. J., Ogren, J.A., "Four years of continuous surface aerosol
1209 measurements from the Department of Energy's Atmospheric Radiation Measurement
1210 Program Southern Great Plains Cloud and Radiation Testbed site," *J. Geophys. Res.*, 106,
1211 20735–20747, 2001.
- 1212 Sheridan, P.J., Jefferson, A., Ogren, J.A., "Spatial variability of submicrometer aerosol radiative
1213 properties over the Indian Ocean during INDOEX," *J. Geophys. Res.*, 107, D19, 8011,
1214 10.1029/2000JD000166, 2002.
- 1215 Sherman, J. P., Sheridan, P. J., Ogren, J. A., Andrews, E., Hageman, D., Schmeisser, L.,
1216 Jefferson, A., and Sharma, S.: A multi-year study of lower tropospheric aerosol variability and
1217 systematic relationships from four North American regions, *Atmos. Chem. Phys.*, 15, 12487–
1218 12517, doi:10.5194/acp-15-12487-2015, 2015.
- 1219 Shinozuka, Y., Redemann, J., Livingston, J. M., Russell, P. B., Clarke, A. D., Howell, S. G.,
1220 Freitag, S., O'Neill, N. T., Reid, E. A., Johnson, R., Ramachandran, S., McNaughton, C. S.,
1221 Kapustin, V. N., Brekhovskikh, V., Holben, B. N., and McArthur, L. J. B.: Airborne observation
1222 of aerosol optical depth during ARCTAS: vertical profiles, inter-comparison and fine-mode
1223 fraction, *Atmos. Chem. Phys.*, 11, 3673–3688, 2011.
- 1224 Sinha, P., Hobbs, P.V., Yokelson, R.J., Bertschi, I.T., Blake, D.R., Simpson, I., Gao, S.,
1225 Kirchstetter, T.W., Novakov, T., "Emissions of trace gases and particles from savanna fires in
1226 southern Africa," *J. Geophys. Res.*, 108, 8487, doi:10.1029/2002JD002325, 2003.
- 1227 Skeie, R. B., T. Berntsen, G. Myhre, C. A. Pedersen, J. Ström, S. Gerland, and J. A. Ogren,
1228 "Black carbon in the atmosphere and snow, from pre-industrial times until present," *Atmos.*
1229 *Chem. Phys.*, 11, 6809–6836, doi:10.5194/acp-11-6809-2011, 2011.
- 1230 Smirnov, A., B. N. Holben, T. F. Eck, O. Dubovik, and I. Slutsker, "Cloud screening and quality
1231 control algorithms for the AERONET database," *Remote Sens. Environ.*, 73, 337– 349, 2000.
- 1232 Subramanian, R., Roden, C. A., Boparai, P., and Bond, T. C.: Yellow beads and missing
1233 particles: Trouble ahead for filter-based absorption measurements, *Aerosol Sci. Technol.*,
1234 41(6), 630–637, DOI: 10.1080/02786820701344589, 2007.
- 1235 Taubman, B.F., Hains, J.C., Thompson, A.M., Marufu, L.T., Doddridge, B.G., Stehr, J.W., Piety,
1236 C.A., and Dickerson, R.R., "Aircraft vertical profiles of trace gas and aerosol pollution over
1237 the mid-Atlantic United States: Statistics and meteorological cluster analysis," *J. Geophys.*
1238 *Res.*, 111, D10S07, doi:10.1029/2005JD006196, 2006.



- 1239 Virkkula, A.: Correction of the Calibration of the 3-wavelength Particle Soot Absorption
1240 Photometer (3 PSAP), *Aerosol Sci. Technol.*, 44, 706–712, 2010.
- 1241 Wang, R., et al., “Estimation of global black carbon direct radiative forcing and its uncertainty
1242 constrained by observations,” *J. Geophys. Res. Atmos.*, 121, 5948–5971,
1243 doi:10.1002/2015JD024326, 2016.
- 1244 Wang, X., Heald, C.L, Ridley, D.A., Schwarz, J.P., Spackman, J.R., Perring, A.E., Coe, H., Liu,
1245 D., Clarke, A.D., “Exploiting simultaneous observational constraints on mass and absorption
1246 to estimate the global direct radiative forcing of black carbon and brown carbon,” *Atmos.*
1247 *Chem. Phys.*, 14, 10989–11010, 2014.
- 1248

1249 **Tables**

1250

1251

1252

1253

1254 **Table 1** Statistical values (medians, means and standard deviations) of AERONET versus in-
 1255 situ comparison where there was an AERONET retrieval within +/-3 h of the end of a 2 h flight
 1256 profile. AERONET values are for Level-1.5 data when there was a Level-2 AOD value and an
 1257 almucantar retrieval. (First value in each cell is median; second set of values in each cell are
 1258 mean± Std.Dev)

| | BND | | SGP | |
|------|-----------------------|-----------------------|-----------------------|-----------------------|
| | AERONET | In-situ | AERONET | In-situ |
| AOD | 0.112; 0.131±0.087 | 0.125; 0.127±0.095 | 0.175; 0.188±0.109 | 0.198; 0.195±0.106 |
| AAOD | 0.010; 0.012±0.007 | 0.003; 0.005±0.006 | 0.025; 0.026±0.011 | 0.005; 0.006±0.004 |
| SSA | 0.906; 0.904±0.036 | 0.967; 0.967±0.016 | 0.854; 0.848±0.041 | 0.971; 0.972±0.011 |

1259

1260

1261

1262 **Table 2** Number of AERONET/IN-SITU AOD and AAOD matches as a function of AERONET
 1263 match criteria and the +/- 3h time window.

1264

| | BND (2006-2009) | SGP(2005-2007) |
|--|-----------------|----------------|
| 1265 Total profile flights | 402 | 171 |
| 1266 Level-2 AOD | 72 | 40 |
| 1267 Level-2 AOD+almucantar retrieval | 56 | 29 |
| 1268 Level-2 AOD+almucantar retrieval+AOD ₄₄₀ >0.20 | 6 | 7 |
| 1269 Level-1.5* AAOD | 24 | 14 |
| 1270 Level-1.5* AAOD + AOD ₄₄₀ >0.20 | 6 | 7 |
| 1271 Level-2 AAOD | 2 | 4 |

1272

1273



Table 3 Direct AAOD comparisons – AERONET ("RS") vs In-Situ ("IS")

| Study, # profiles Citation(s) | Location, aerosol type AOD comments | Instruments corrections size cut | AAOD comparison information | Comments |
|---|---|--|--|--|
| BND 24 profiles This study | Central US Rural, continental AOD ₄₄₀ range: 0.04-0.55 AOD comparison See Fig. 3a | PSAP-3wave TSI neph-3wave B1999, O2010, AO1998 f(RH) adjust Dp<5-7 μm | Wavelength=440, 670 nm Ångström interpolation RS AAOD>IS AAOD AAOD ₄₄₀ range: 0.001-0.042 | Profiles matched within 3 hours of AERONET measurement. Profiles within 15 km of AERONET measurement. Used AERONET 1.5 AAOD values for cases with valid AERONET 2.0 AOD value. |
| SGP 14 profiles This study | Central US Rural, continental AOD ₄₄₀ range: 0.06-0.43 AOD comparison See Fig. 3b | PSAP-3wave TSI neph-3wave B1999, O2010, AO1998 f(RH) adjust Dp<5-7 μm | Wavelength=440, 670 nm Ångström interpolation RS AAOD>IS AAOD AAOD ₄₄₀ range: 0.012-0.052 | Profiles matched within 3 hours of AERONET measurement. Profiles within 1 km of AERONET measurement Used AERONET 1.5 AAOD values for cases with valid AERONET 2.0 AOD value. |
| MAC 13 profiles Corrigan et al., 2008 | Indian Ocean Pollution AOD ₄₄₀ range: 0.1-0.6 No AOD comparison | Aethalometer 3-wave OPC +Mie for scattering A2005 Dp<5 μm | Wavelength not provided RS AAOD>IS AAOD AAOD ₄₄₀ range: 0.005-0.033 | No details on how profiles matched with retrievals in terms of time or distance. No details on version of AERONET data used; this is relevant, given low AODs in first half of study – not sure if there were comparisons for low AODs. Note: this study is the one cited by Bond et al. (2013) to support the use of AERONET to scale modeled BC values |



In-situ instrument corrections: B1999=Bond et al., 1999; O2010=Ogren, 2010, AO1998=Anderson and Ogren, 1998; A2005=Arnott et al., 2005; Ångström interpolation – indicates in-situ wavelength adjusted to AERONET wavelength using Ångström interpolation; f(RH) adjust – indicates the in-situ measurements were adjusted to ambient humidity conditions for the AOD comparison. IS=In-situ measurements, RS=Remote sensing (AERONET) measurements

Table 4 SSA comparisons – AERONET vs In-situ

| Study, # profiles Citation(s) | Location, aerosol type AOD comments | Instruments, Corrections, Inlet size cut | SSA comparison information | Comments |
|--|--|--|---|---|
| BND 24 profiles This study | Central US Rural, continental AOD ₄₄₀ range: 0.04-0.55 AOD comparison: See Fig. 2a | PSAP-3wave TSI neph-3wave B1999, O2010, AO1998 f(RH) adjust Dp<5-7 μm | Wavelength=440, 670 nm Ångström interpolation RS SSA<IS SSA | Profiles matched within 3 hours of AERONET measurement. Profiles within 15 km of AERONET measurement. Used AERONET 1.5 AAOD values for cases with valid AERONET 2.0 AOD value. |
| SGP 14 profiles This study | Central US Rural, continental AOD ₄₄₀ range: 0.06-0.43 AOD comparison: See Fig. 2b | PSAP-3wave TSI neph-3wave B1999, O2010, AO1998 f(RH) adjust Dp<5-7 μm | Wavelength=440, 670 nm Ångström interpolation RS SSA<IS SSA | Profiles matched within 3 hours of AERONET measurement. Profiles within 1 km of AERONET measurement. Used AERONET 1.5 AAOD values for cases with valid AERONET 2.0 AOD value. |
| AAO (BND) 1 profile Esteve et al., 2012 | Central US Rural, continental AOD ₅₅₀ = 0.65 AOD comparison: | PSAP-3wave TSI neph-3wave B1999, O2010, AO1998 f(RH) adjust | Wavelength=550 nm Power law interpolation RS SSA < IS SSA | Profiles matched within 2 hours of AERONET measurement. Profiles within 15 km of AERONET measurement. Used AERONET 2.0 AOD value. |



| | RS AOD>IS AOD | Dp<5-7 μm | | |
|--|---|--|--|--|
| DISCOVER-AQ 12 profiles Schafer et al., 2014 | East Coast US Polluted air AOD ₄₄₀ >0.2 AOD compare: RS AOD > IS AOD (by 23%)* | PSAP-3wave TSI neph-3wave V2010, AO1998* f(RH) adjust Dp<4 μm * | Wavelength=550 nm AERONET "interpolated" to 550 (no detail provided) In-situ absorption interpolated to 550 using Ångström interpolation RS SSA < IS SSA | Profile matched within 45 min of AERONET measurement. Profile within 1 km of AERONET measurement. Used AERONET 2.0 Altitude range: at least <500 m and >1500 m, min and max altitudes: 367 m and 3339 m |
| CLAMS 1 profile Magi et al., 2005 | East Coast US Polluted air AOD ₄₄₀ =0.60 AOD comparison: RS AOD > IS AOD (by 15%) | PSAP-1wave MSE neph-3wave B1999, AO1998 f(RH) adjust Inlet size cut not reported, Sinha, 2003 suggests Dp<4 μm | Wavelength=550 nm Wave_adj =quadratic polynomial interpolation RS SSA < IS SSA | Profile matched within 1 hour of AERONET measurement. Profile within 3 km of AERONET measurement. Used AERONET 2.0 AOD ₄₄₀ from http://aeronet.gsfc.nasa.gov/ , not stated in paper. Also compared campaign AERONET average with profile average: SSA's much closer, but profiles weren't necessarily close in time or space to AERONET site |
| ESCOMPTE 1 profile Mallet et al., 2005 | Avignon, France Pollution AOD ₄₄₀ >0.55 No AOD comparison | PSAP-1wave TSI neph-3wave B1999, A1999 No f(RH) adj Inlet Dp not given | Wavelength=550 nm Wave_adj = estimated from visual inspection (spectral dependence is relatively flat) RS SSA < IS SSA | Profile matched within 1 hour of AERONET measurement. Profile within 10 km of AERONET measurement. Used AERONET 2.0 AOD ₄₄₀ from http://aeronet.gsfc.nasa.gov/ , not stated in paper. Did not adjust in-situ measurements for |



| | | | | |
|---|--|---|--|--|
| | | | | f(RH), so presumably IS SSA would increase so it was even larger than RS SSA. |
| SAFARI 5 profiles Leahy et al., 2007 UW plane | Southern Africa Biomass burning AOD ₅₅₀ >0.28-1.12 AOD comparison: RS AOD > IS AOD RS=1.12*IS-0.05 R ² =0.99 | PSAP-1wave MSE neph-3wave B1999;H2000 f(RH) adjust Dp<4 μm | Wavelength=550 nm Wave_adj= 2nd order polynomial For AOD ₅₅₀ >0.6 (3 profiles) RS SSA > IS SSA For AOD ₅₅₀ <0.3 (2 profiles) RS SSA ≤ IS SSA | Profiles matched within 1-4 hours of AERONET measurement. Profiles within 20 km of AERONET measurement. Used AERONET 2.0 Also found: AEROCOM model>insitu |
| SAFARI 1 profile Haywood et al, 2003 C-130 | Southern Africa Biomass burning AOD ₄₄₀ =0.71 AOD comparison: RS AOD < IS AOD | PSAP-1wave TSI neph-3wave B1999,AO1998 No f(RH) adj Dp<2-4 μm | Wavelength= native Wave_adj = none RS SSA < IS SSA | Profile matched within 2 hours of AERONET measurement. Profiles within 10 km of AERONET measurement. Used AERONET 2.0 They defend the lack of f(RH) correction because (a) ambient RH values < 56% and (b) previous measurements of f(RH) of BB aerosol suggest minimal hygroscopicity Paper mostly focused on size dist comparison; SSA comparison seems like afterthought. |
| DABEX 3 profiles Osborne et al., 2008 | Africa Dust/BB AOD comparison RS AOD < IS AOD (by up to 40%) AOD ₅₅₀ ~0.3-0.6 | PSAP-1wave TSI neph-3wave B1999,AO1998 No f(RH) adj Dp<2-4 μm | Wavelength=550 nm Wave_adj=log interpolation RS SSA < IS SSA | No details on how profiles matched with retrievals in terms of time. Profiles within 100 km of AERONET measurement Used AERONET 2.0 They defend the lack of f(RH) correction because (a) ambient RH values are mostly |



| | | | | |
|----------------------|--|--|---|--|
| | | | | <p>low (<60%) and (b) previous measurements of f(RH) of BB aerosol suggest minimal hygroscopicity</p> <p>Jan 21, 23 and 30 profiles IS overpredicts AOD so IS SSA is greater than RS SSA</p> <p>Suggest it could be due to large particle correction to IS measurements using PCASP. McConnell et al., (2008) suggests problems with nephelometer sensitivity</p> |
| DABEX 1 profile | Africa DUST/BB | PSAP-1wave TSI neph-3wave | Wavelength=550 nm Wave_adj=log interpolation | <p>Profile matched within 1 hour of AERONET measurement. Profile within 100 km of AERONET measurement</p> <p>Used AERONET 2.0</p> <p>They defend the lack of f(RH) correction because ambient RH values are mostly low (<40% with a max of 70%)</p> <p>Jan 19 profile</p> <p>Incorrectly used Mie to adjust σ_{ap} to 550 after B1999 applied</p> |
| Johnson et al., 2009 | AOD comparison: RS AOD < IS AOD (by ~10%) AOD ₅₅₀ > 0.7 | B1999,AO1998 No f(RH) adj Dp<2-4 μm | RS SSA < IS SSA | |

IS=In-situ measurements, RS=Remote sensing (AERONET) measurements. In-situ instrument corrections: B1999=Bond et al., 1999; V2010=Virkula et al., 2010; O2010=Ogren, 2010; AO1998=Anderson and Ogren, 1998; H2000=Hartley et al., 2000; A2005=Arnott et al., 2005; Ångström interpolation – indicates wavelength adjustment using Ångström exponent interpolation; f(RH) adjust – indicates the in-situ measurements were adjusted to ambient humidity conditions for the AOD and SSA comparison.

[†]Information about Discover-AQ flights from Crumreynrolle et al. (2014)



Figures

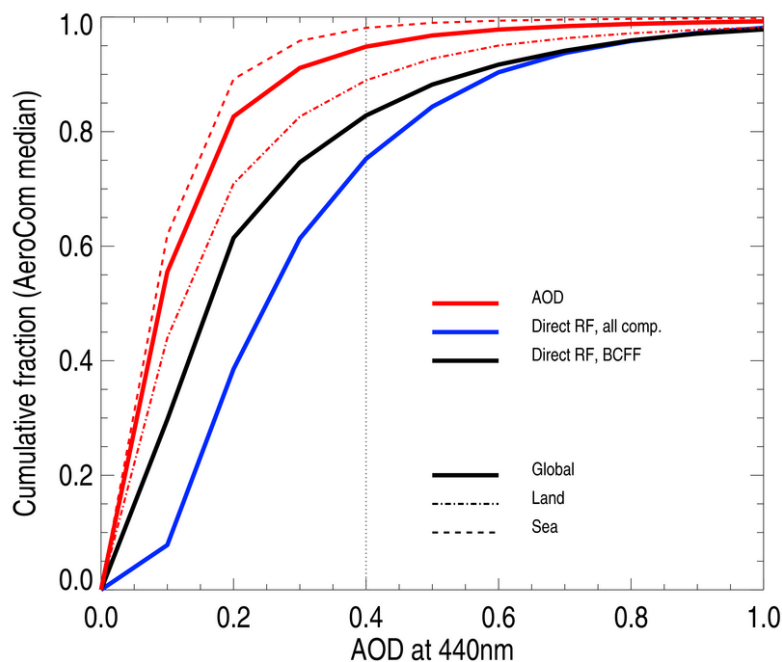


Figure 1. Cumulative AOD_{440} frequency distribution (red lines) based on output from five AeroCom models. Blue and black lines show contribution of total aerosol and fossil fuel black carbon, respectively, to the global radiation budget as a function of AOD_{440} . See text for details. Models used to generate the AOD lines include: GMI-MERRA-v3, GOCART-v4, LMDZ-INCA, OsloCTM2, and SPRINTARS-v385. Models used to generate the radiative forcing lines include all but the GMI-MERRA-v3 model. Model information and references can be found in Myhre et al., (2013).

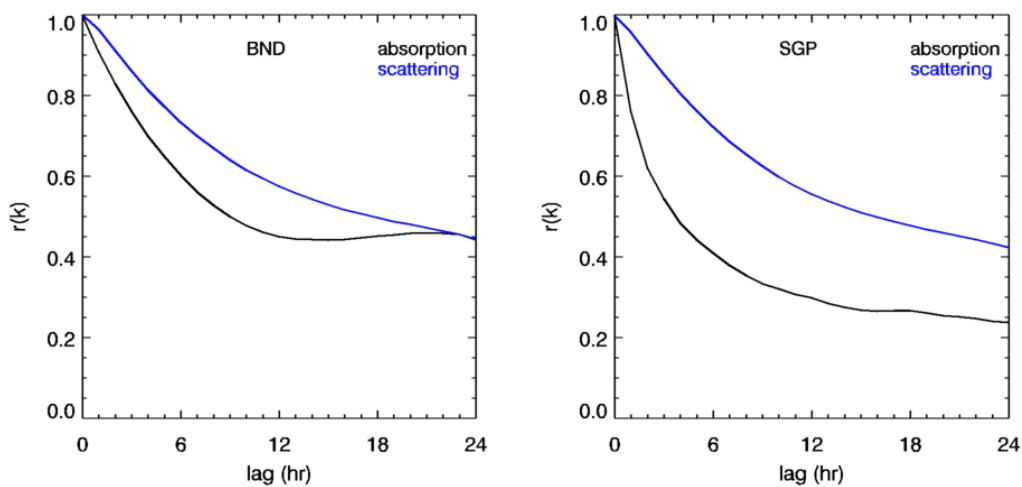


Figure 2. Correlograms for BND and SGP; wavelength = 550 nm, $D_p < 10 \mu\text{m}$, based on hourly averaged surface in-situ data between 1995-2013 (BND) and 1996-2013 (SGP).

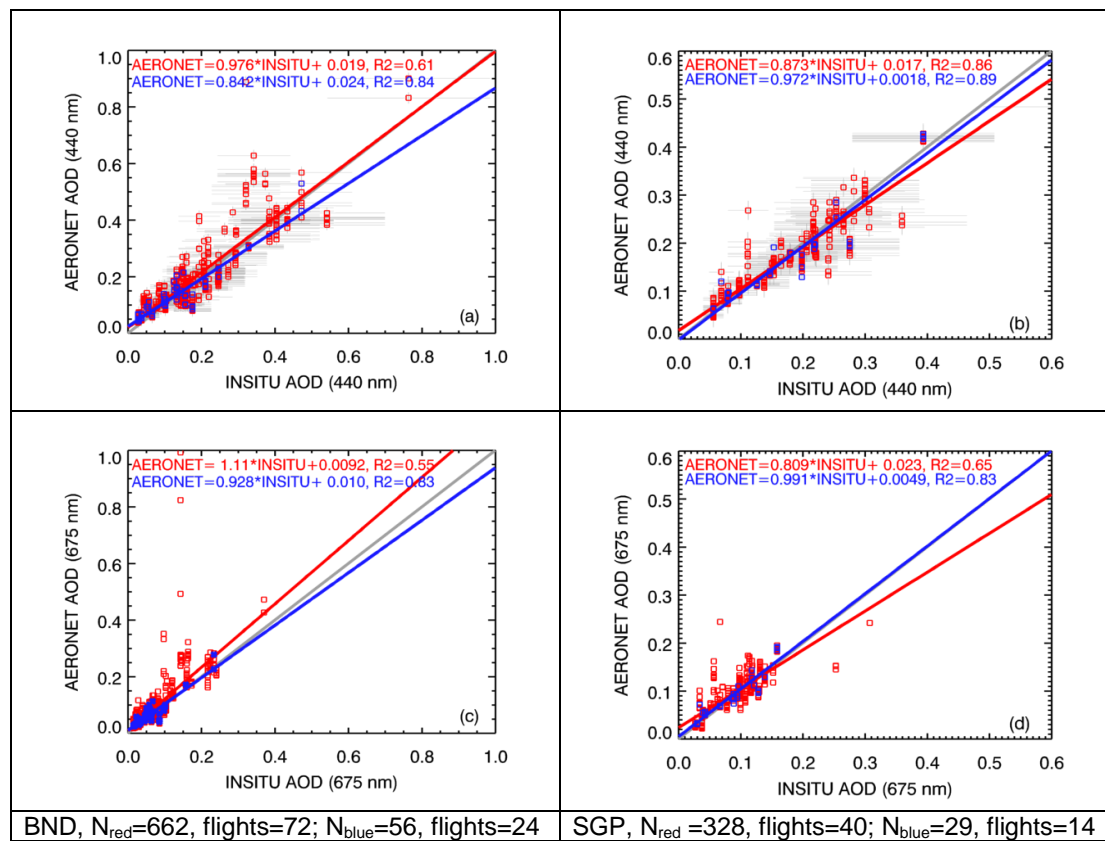


Figure 3. AOD comparison (a) BND at 440 nm; (b) SGP at 440 nm; (c) BND at 675 nm; and (d) SGP at 675 nm; thick gray line is 1 to 1 line. Thin gray lines associated with each data point represent measurement uncertainties. Red points and fit line represent all AERONET direct sun Level-2 AOD measurements within +/-3 hours of end of profile. Blue points and fit line represent AERONET Level-2 AOD measurements with successful almucantar retrievals within +/-3 hours of end of profile.

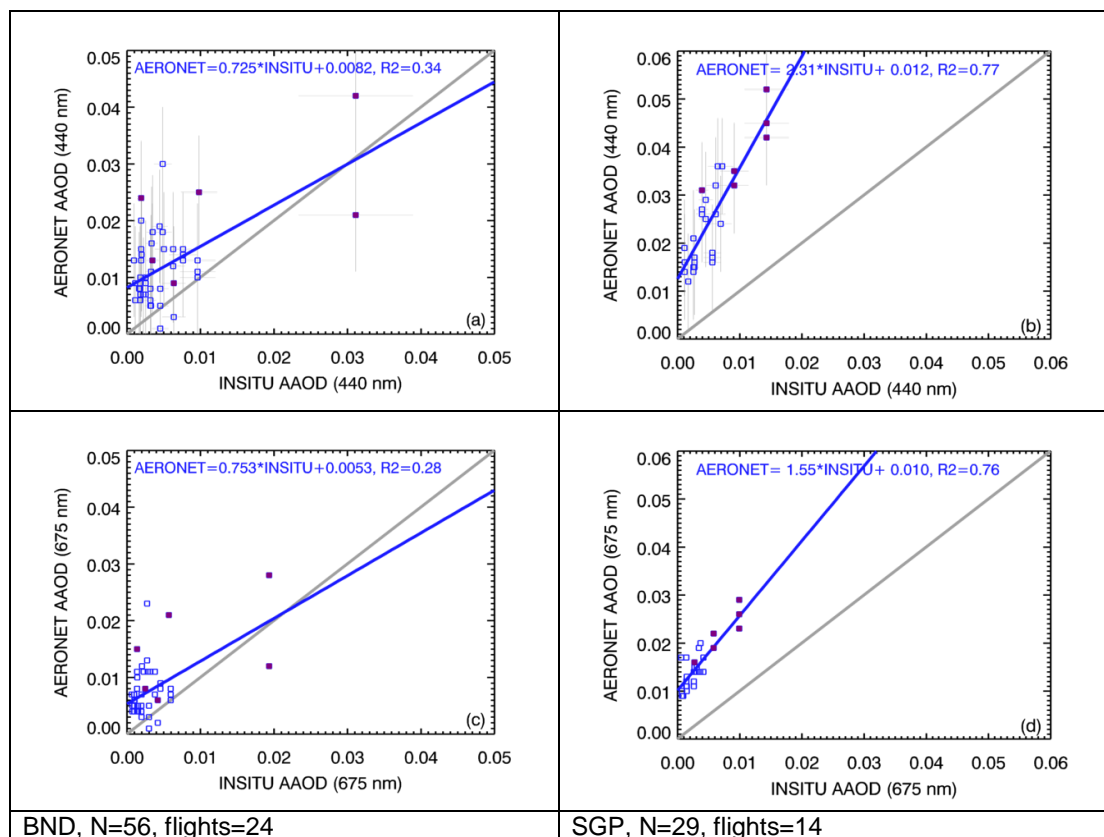


Figure 4. AAOD comparison, (a) BND at 440 nm; (b) SGP at 440 nm ; (c) BND at 675 nm; and (d) SGP at 675 nm. Blue line is linear fit for all points shown; gray line is 1 to 1 line. Thin gray lines associated with each data point represent measurement uncertainties. Points show AERONET Level-1.5 AAOD retrievals for which there was a successful AERONET Level-2 almucantar retrieval within +/-3 hours of end of profile. Purple points indicate the few points for which there are AERONET Level-2 almucantar retrievals and where $AOD_{440} > 0.2$.

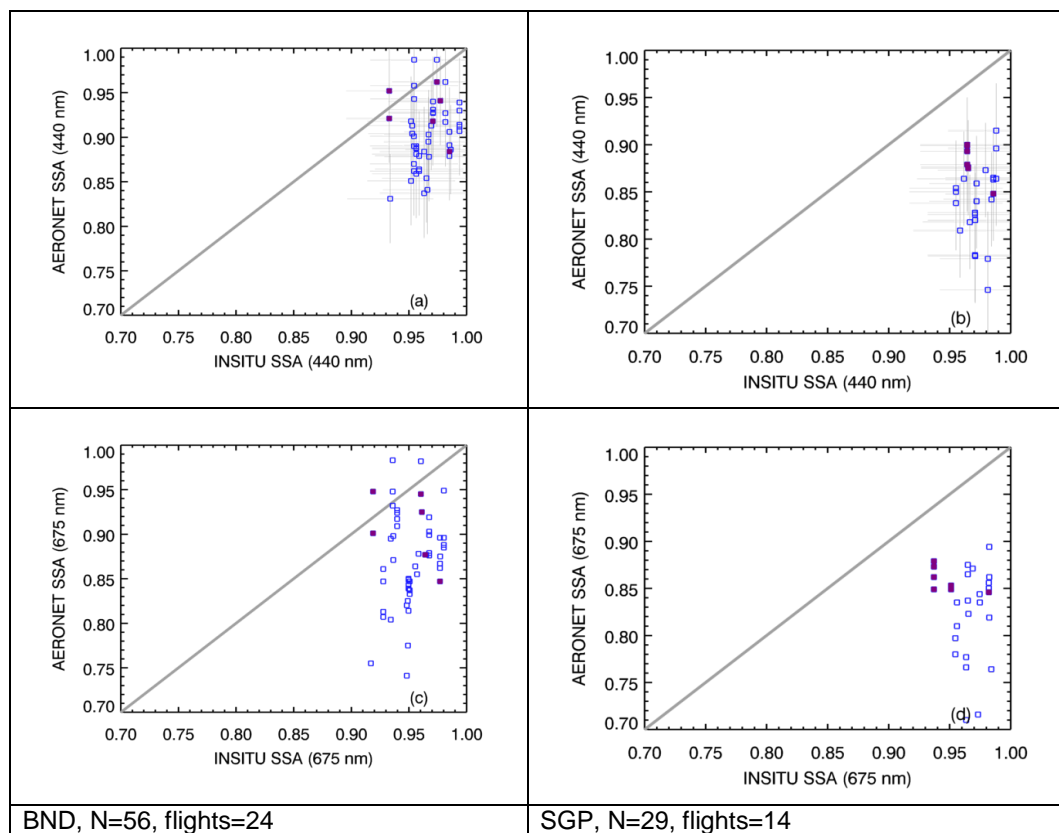


Figure 5. SSA comparison, (a) BND at 440 nm (b) SGP at 440 nm; (c) BND at 675 nm; and (d) SGP at 675 nm. Blue line is linear fit for all points shown; gray line is 1 to 1 line. Thin gray lines associated with each data point represent measurement uncertainties. Points show AERONET Level-1.5 AOD retrievals for which there was a successful AERONET Level-2 almicantar retrieval within +/-3 hours of end of profile. Purple points indicate the few points for which there are AERONET Level-2 almicantar retrievals and where $AOD_{440} > 0.2$.

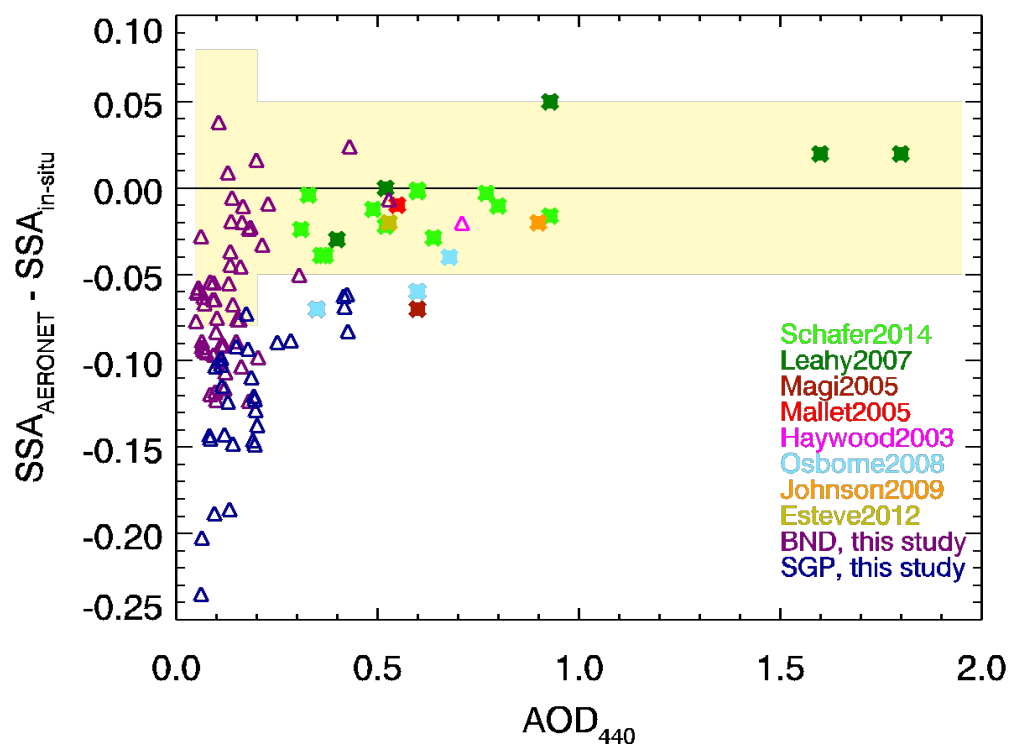


Figure 6. AOD_{440} vs $[SSA_{AERONET} - SSA_{INSITU}]$ for direct comparisons studies listed in Table 4. Open symbols are for SSA_{440} difference; filled symbols are for SSA_{550} difference. AOD_{440} values for Leahy2007, Osborne2008, Johnson2009 use the Level-2 values reported on the AERONET webpage for the locations and dates of the specific profile. Shading indicates combined uncertainty of AERONET SSA values as function of AOD as reported in Table 4 of Dubovik et al. (2000) and uncertainty in the in-situ SSA calculated using equation 2.

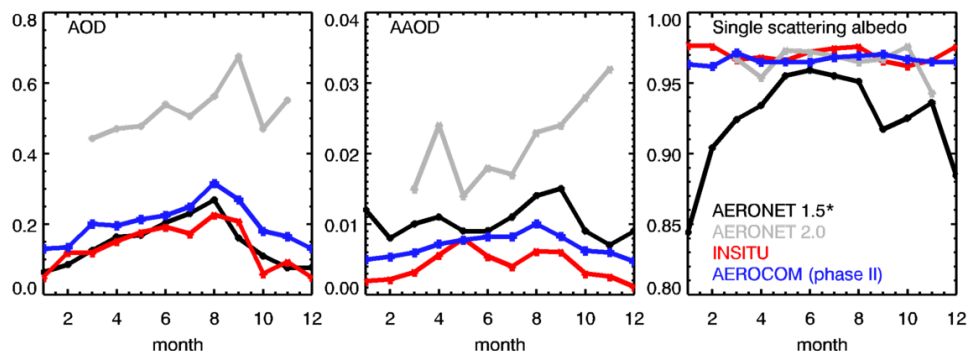


Figure 7a. Monthly medians of BND aerosol optical properties at 440 nm. AERONET medians are for 1996-2011. AERONET AOD medians are for observations with Level-2 almucantar retrievals, with corresponding AAOD and SSA retrievals at Level-1.5 (black) or Level-2 (gray). In-situ data are for June 2006-September 2009. AERONET 2.0 AOD and AAOD values are biased high by definition, because of the $AOD_{440} > 0.4$ constraint. AERONET 2.0 direct sun retrievals (not shown) are similar to the AERONET 1.5 AOD values. In-situ values are derived from 365 flights over BND. AeroCom Phase II median model results cover various time periods (depending on the model) and are reported at 550 nm.

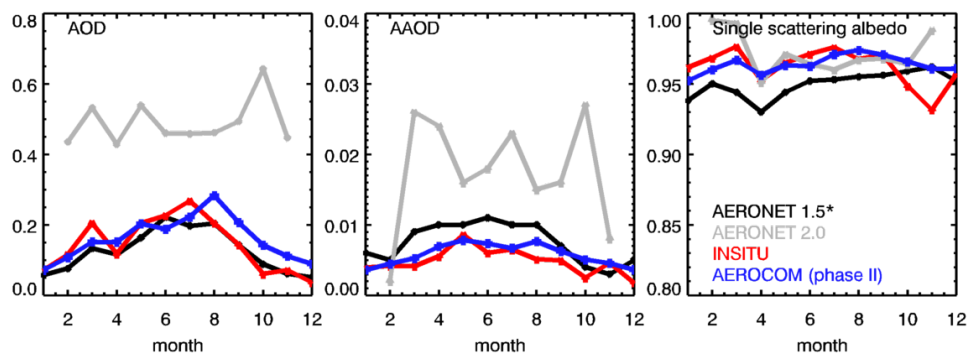


Figure 7b. Monthly medians of SGP aerosol optical properties at 440 nm. AERONET medians are for 1996-2011. In-situ data are for September 2005-December 2007. AERONET AOD medians are for observations with Level-2 almucantar retrievals, with corresponding AAOD and SSA retrievals at Level-1.5 (black) or Level-2 (gray). AERONET 2.0 values are biased high by definition, because of the $AOD_{440} > 0.4$ constraint. AERONET 2.0 direct sun retrievals (not shown) are similar to the AERONET 1.5 AOD values. In-situ values are derived from 322 flights over SGP. AeroCom Phase II median model results cover various time periods (depending on the model) and are reported at 550 nm.

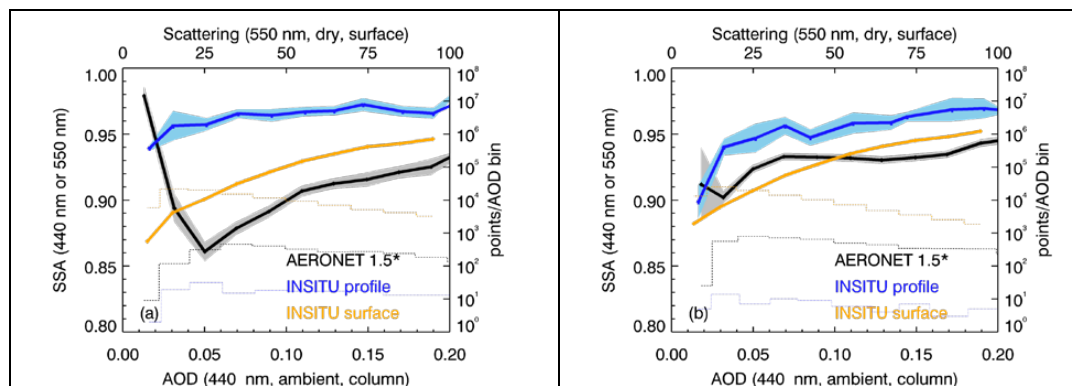


Figure 8. Systematic variability of SSA as a function of loading for (a) BND and (b) SGP for AERONET 1.5* AOD and SSA (black lines), AOD and SSA from in-situ profiles (blue lines) and in-situ scattering and SSA from surface measurements (orange lines). Solid lines indicate mean values of SSA and AOD for each 0.05 AOD bin (10 Mm^{-1} scattering bin). Shaded areas represent mean standard error (mean standard error for surface data is within thickness of orange line). Histograms indicate the number of points in each AOD (or scattering) bin. Plot based on BND and SGP AERONET data (date range: 1996-2012) and BND INSITU profile data (date range: 2006-2012); SGP INSITU profile data (date range: 2006-2007). Surface data (orange lines) are for 550 nm, low RH, hourly in-situ data from the surface sites at BND (date range: 1996-2013) and SGP (date range: 1997-2013). AERONET 1.5* is from Level-1.5 retrievals with a corresponding Level-2 almucantar retrieval.